

# Agricultural and Forest Meteorology

## Assessing the impact of climate and crop diversity on regional greenhouse gas emissions and water demand of cropland

--Manuscript Draft--

<b>Manuscript Number:</b>	
<b>Article Type:</b>	Research Paper
<b>Section/Category:</b>	Plant physiology, Crop Modelling, water relations including evapotranspiration, WUE, interception
<b>Keywords:</b>	GHG; water demand; China; main crop; climate; spatial distribution
<b>Corresponding Author:</b>	Shikun Sun Northwest A&F University Yangling, CHINA
<b>First Author:</b>	yihe tang
<b>Order of Authors:</b>	yihe tang  Shikun Sun  Yuhan Lei  Fei Mo  Chong Li  Jinfeng Zhao  Jiajun Tong  yali yin  Yubao Wang
<b>Abstract:</b>	To tackle the challenges of climate warming and freshwater scarcity, evaluating greenhouse gas (GHG) emissions and water demand in agricultural production can contribute positively to sustainable agricultural practices. This study aimed to quantify the greenhouse gas emissions and water requirements of three major food crops in diverse environmental and regions in China, with a specific focus on exploring their spatial heterogeneity due to regional differences. The parameterized DNDC model was employed to quantify crop GHG emissions, while the Penman-Monteith formula, coupled with modified crop coefficients, was utilized to assess water demand. The result showed that the total GHG emission of major crops in China was 372.43 Tg/yr (CO <sub>2</sub> ), 11.68 Tg/yr (CH <sub>4</sub> ), 475.56 Gg/yr (N <sub>2</sub> O) respectively; and the water demand was 473.60 Gm <sup>3</sup> , in 2015. The Middle-lower Yangtze Plain (MLYP) had the highest water-carbon fluxes. High-temperature and high-precipitation regions had greater GHG emission intensity; the intensity of different GHG emissions was significantly influenced by the type of crops. Late rice had the highest emission intensity. The geospatial distribution of GHG emissions and water demand displayed opposite patterns, with meteorological conditions and crop types as the main reasons. Soil bulk density was the most significant soil element influencing regional fluxes. These results will help to assess the spatial heterogeneity of agricultural water and carbon, and the quantitative results can be used as evaluation indicators to establish environmentally friendly agricultural cropping patterns suitable for different cropping regions.
<b>Suggested Reviewers:</b>	Sien Li Professor, China Agricultural University lisien@cau.edu.cn  Feng Zhang Professor, Lanzhou University zhangfeng@lzu.edu.cn Current maintainer of the model used  Allan Andales

Colorado State University  
Allan.Andales@ColoState.edu

jing liu  
Hohai University  
liujing0027@hhu.edu.cn

Zhongkui Luo  
Zhejiang University  
luozk@zju.edu.cn

Dear editor,

We are submitting a manuscript entitled “*Assessing the impact of climate and crop diversity on regional greenhouse gas emissions and water demand of cropland*” for your consideration for publication as a communication in *Agricultural and Forest Meteorology*.

**In this study, we did the following work:**

This study quantified the greenhouse gas (GHG) emissions and crop water requirements in 337 cities in China for three major grains: corn, wheat (winter wheat, spring wheat), rice (single-cropping rice, early rice, and late rice) to assess the GHG emissions and water demand of cropland in China. Herein, the GHG emissions and water demand in city level, province level, agricultural region level and country level were assessed; the influence of regional differences in environmental elements, especially the main meteorological elements, on the spatial distribution characteristics of agricultural water carbon intensity was determined; and a sensitivity analysis of the main factors affecting GHG emissions was conducted. The results of this study will help to assess the inter-crop and spatial heterogeneity of water-carbon fluxes, and the quantitative results can be used as evaluation indicators to establish environmentally friendly agricultural cropping patterns suitable for different cropping regions.

This study analyzed three major crops with extensive coverage and universality in China. It offers an integrated assessment of two crucial agricultural elements: "water" and "carbon." The topic aligns with the publication requirements of this journal.

This work was jointly supported by the National Natural Science Foundation of China (52122903, 51979230), Science Fund for Distinguished Young Scholars of Shaanxi Province(2021JC20), Fok Ying-Tong Education Foundation (171113) and Cyrus Tang Foundation, China National Postdoctoral Program for Innovative Talents (BX20220255).

**Author identifying information:**

Yihe Tang <sup>1,2,3</sup>, Shikun Sun <sup>1,2,3\*</sup>, Yuhan Lei <sup>1,2,3</sup>, Fei Mo <sup>4</sup>, Chong Li <sup>1,2,3</sup>, Jinfeng Zhao <sup>1,2,3</sup>, Jiajun Tong <sup>1,2,3</sup>, Yali Yin <sup>1,2,3</sup>, Yubao Wang <sup>1,2,3</sup>

<sup>1</sup> Key Laboratory of Agricultural Soil and Water Engineering in Arid and Semiarid Areas, Ministry of

Education, Northwest A&F University, Yangling 712100, Shaanxi, China

<sup>2</sup> Institute of Water Saving Agriculture in Arid regions of China, Northwest A&F University, Yangling

712100, Shaanxi, China

<sup>3</sup> National Engineering Research Center for Water Saving Irrigation at Yangling, Yangling 712100,

Shaanxi, China

<sup>4</sup> College of Agronomy, Northwest A&F University, Yangling, 712100, Shaanxi, China

Thank you for your consideration of our work. We look forward to your suggestions for improving the quality of our work.

With best regards,

Yihe Tang

Institute of Water Saving Agriculture in Arid regions of China, Northwest A&F University,  
Yangling 712100, Shaanxi, China

Key Laboratory of Agricultural Soil and Water Engineering in Arid and Semiarid Areas, Ministry of  
Education, Northwest A&F University

E-mail addresses: [tangyh@nwafu.edu.cn](mailto:tangyh@nwafu.edu.cn)

Dear editor,

We are submitting a manuscript entitled “*Spatial heterogeneity of greenhouse gas emissions and water demand on major farmland in China*” for your consideration for publication as a communication in *Agricultural Systems*.

**In this study, we did the following work:**

This study quantified the GHG emissions and crop water requirements in 337 cities in China for six major grains: maize, winter wheat, spring wheat, single-cropping rice, early rice, and late rice, to assess the water-carbon effect of cultivation in China. Herein, the GHG emissions and water requirements in different provinces and agricultural regions were assessed; the water carbon intensity in different provinces and agricultural regions was examined; the influence of regional differences in environmental elements, especially the main meteorological elements, on the spatial distribution characteristics of agricultural water carbon intensity was determined; and a sensitivity analysis of the main factors affecting GHG emissions was conducted.

The results of this study will help to assess the inter-crop and spatial heterogeneity of water-carbon fluxes, and the quantitative results can be used as evaluation indicators to establish environmentally friendly agricultural cropping patterns suitable for different cropping regions.

This study analyzed six kinds of crops, which has a large coverage and universality in China, and the topic meets the publication requirements of this journal.

This work was jointly supported by the National Natural Science Foundation of China (52122903, 51979230), Science Fund for Distinguished Young Scholars of Shaanxi Province(2021JC20), Fok Ying-Tong Education Foundation (171113) and Cyrus Tang Foundation, China National Postdoctoral Program for Innovative Talents (BX20220255).

**Author identifying information:**

Yihe Tang <sup>1,2,3</sup>, Shikun Sun <sup>1,2,3\*</sup>, Yuhua Lei <sup>1,2,3</sup>, Fei Mo <sup>4</sup>, Chong Li <sup>1,2,3</sup>, Jinfeng Zhao <sup>1,2,3</sup>, Jiajun Tong <sup>1,2,3</sup>, Yali Yin <sup>1,2,3</sup>, Yubao Wang <sup>1,2,3</sup>

<sup>1</sup> Key Laboratory of Agricultural Soil and Water Engineering in Arid and Semiarid Areas, Ministry of Education, Northwest A&F University, Yangling 712100, Shaanxi, China

<sup>2</sup> Institute of Water Saving Agriculture in Arid regions of China, Northwest A&F University, Yangling 712100, Shaanxi, China

<sup>3</sup> National Engineering Research Center for Water Saving Irrigation at Yangling, Yangling 712100, Shaanxi, China

<sup>4</sup> College of Agronomy, Northwest A&F University, Yangling, 712100, Shaanxi, China

Thank you for your consideration of our work. We look forward to your suggestions for improving the quality of our work.

With best regards,

Yihe Tang

Institute of Water Saving Agriculture in Arid regions of China, Northwest A&F University, Yangling 712100, Shaanxi, China

Key Laboratory of Agricultural Soil and Water Engineering in Arid and Semiarid Areas, Ministry of Education, Northwest A&F University

E-mail addresses: [tangyh@nwafu.edu.cn](mailto:tangyh@nwafu.edu.cn)

# Assessing the impact of climate and crop diversity on regional greenhouse gas emissions and water demand of cropland

Yihe Tang<sup>1,2,3</sup>, Shikun Sun<sup>1,2,3\*</sup>, Yuhua Lei<sup>1,2,3</sup>, Fei Mo<sup>4</sup>, Jinfeng Zhao<sup>1,2,3</sup>, Chong Li<sup>1,2,3</sup>, Jiajun Tong<sup>1,2,3</sup>, Yali Yin<sup>1,2,3</sup>, Yubao Wang<sup>1,2,3</sup>

<sup>1</sup> Key Laboratory of Agricultural Soil and Water Engineering in Arid and Semi-arid Areas, Ministry of Education, Northwest A&F University, Yangling 712100, Shaanxi, China

<sup>2</sup> Institute of Water Saving Agriculture in Arid regions of China, Northwest A&F University, Yangling

<sup>3</sup> National Engineering Research Center for Water Saving Irrigation at Yangling, Yangling 712100, Shaanxi, China.

12 <sup>4</sup> College of Agronomy, Northwest A&F University, Yangling, 712100, Shaanxi, China

\*Corresponding author: Sun SK([sksun@nwafu.edu.cn](mailto:sksun@nwafu.edu.cn))

14 College of Water Resources and Architectural Engineering, Northwest A&F University, Yangling 712100,  
15 P. R. China

16     **Abstract**

17         To tackle the challenges of climate warming and freshwater scarcity, evaluating greenhouse gas  
18         (GHG) emissions and water demand in agricultural production can contribute positively to sustainable  
19         agricultural practices. This study aimed to quantify the greenhouse gas emissions and water requirements  
20         of three major food crops in diverse environmental and regions in China, with a specific focus on  
21         exploring their spatial heterogeneity due to regional differences. The parameterized DNDC model was  
22         employed to quantify crop GHG emissions, while the Penman-Monteith formula, coupled with modified  
23         crop coefficients, was utilized to assess water demand. The result showed that the total GHG emission  
24         of major crops in China was 372.43 Tg/yr ( $\text{CO}_2$ ), 11.68 Tg/yr ( $\text{CH}_4$ ), 475.56 Gg/yr ( $\text{N}_2\text{O}$ ) respectively;  
25         and the water demand was 473.60  $\text{Gm}^3$ , in 2015. The Middle-lower Yangtze Plain (MLYP) had the  
26         highest water-carbon fluxes. High-temperature and high-precipitation regions had greater GHG emission  
27         intensity; the intensity of different GHG emissions was significantly influenced by the type of crops.  
28         Late rice had the highest emission intensity. The geospatial distribution of GHG emissions and water  
29         demand displayed opposite patterns, with meteorological conditions and crop types as the main reasons.  
30         Soil bulk density was the most significant soil element influencing regional fluxes. These results will  
31         help to assess the spatial heterogeneity of agricultural water and carbon, and the quantitative results can  
32         be used as evaluation indicators to establish environmentally friendly agricultural cropping patterns  
33         suitable for different cropping regions.

34  
35         **Keywords:** GHG; water demand; China; main crop; climate; spatial distribution  
36

37     **1. Introduction**

38       Agricultural production plays an important role in food security. The soil emits large amounts of  
39       greenhouse gases (GHGs) into the atmosphere and consumes large amounts of water due to crop  
40       cultivation and human interference. China's GHG emissions from the agricultural sector are equivalent  
41       to 828 million tons of carbon dioxide equivalent(MEEPBC, 2019) and in 2021, the agricultural water  
42       consumption was 364.43 billion m<sup>3</sup> (MWRPRC, 2021). Notably, 17% of the land in China is used for  
43       crop cultivation(NBS, 2020). Agricultural soils emit large amounts of carbon dioxide (CO<sub>2</sub>), methane  
44       (CH<sub>4</sub>), and nitrous oxide (N<sub>2</sub>O), the three most important GHGs, ultimately accounting for 13% of the  
45       total emissions. CH<sub>4</sub> and N<sub>2</sub>O are important GHGs from agricultural sources, N<sub>2</sub>O and methane CH<sub>4</sub>  
46       emissions and contributed 25%–30% of total N<sub>2</sub>O emissions and 40%–50% of total CH<sub>4</sub> emissions  
47       during the 2000s(Tian et al., 2014).

48       Corresponding to emissions, agriculture consumes 70% of the world's total water resources (Postel  
49       et al., 2004). Further, China uses only 6.5% of the world's fresh water to feed 21% of the world's  
50       population(UNOHCHR, 2010). Accordingly, the problem of water scarcity is severe. The distribution of  
51       water resources has obvious spatial variability, with uneven distribution in the humid south and arid north,  
52       and differences in the distribution of water resources in intermediate areas located in the transition  
53       zone(Piao et al., 2010). Different crops have different water demand(Pereira et al., 2021), and spatial  
54       differences in water resources and climatic characteristics directly affect the planting structure of crops.

55       China has a large latitudinal span, and the characteristics of agricultural production significantly  
56       differ among agricultural regions. Different climatic and soil conditions affect crop growth, thereby  
57       impacting water and carbon fluxes in many ways. By affecting the spatial and temporal distribution of  
58       water resources (Lu et al., 2019), the potential evapotranspiration of crops, soil moisture, and nutrients  
59       can cause differences in GHG emissions and water demand between regions. Different crops have  
60       different emission effects and water demand during the growth period owing to differences in their  
61       physiological characteristics and other aspects(Pereira et al., 2021; Zhang et al., 2020). This difference  
62       is manifested based on their influence on the regional agricultural cropping structure and crop  
63       phenology(Mo et al., 2013), which causes differences in GHG emissions and water demand between  
64       different crops. Analyzing the factors that efficiently contribute to water conservation and emission  
65       reduction in agriculture is thus an important topic.

66       The water and carbon cycles of agroecosystems are not independent of each other but are closely  
67       linked and coupled with each other. These two cycle systems are driven by the regional environment,  
68       agricultural production inputs, and other factors(W. Yan et al., 2021), and have interrelationships in  
69       spatial distribution. With various conflicts, such as global warming and water scarcity, a comprehensive

1 assessment of the water-carbon effect of farmland under different environmental conditions should be  
2 carried out to determine whether farming is sustainable.  
3

4 Most methods for assessing agricultural water carbon, especially GHG emissions in large regions,  
5 rely on simple linear methods. The commonly used methods include IPCC method, emission factor  
6 method, life cycle method, and modeling method(Della Chiesa et al., 2022; Yang et al., 2021; Wang et  
7 al., 2021). Climate, soil, crop type, and farm management practices are important drivers of GHG  
8 emission intensity. Model simulations allow full consideration of the impact of these factors on the water-  
9 carbon effect, thereby providing a fundamental tool for assessing differences across regions and climatic  
10 conditions. The denitrification decomposition (DNDC) model developed by Li et al. (Li et al., 1992) is  
11 a process-based biochemical model that focuses on C and N cycling in agroecosystems and can simulate  
12 a wide range of GHGs for different crops. Point(Foltz et al., 2019; Shi et al., 2021; Zhao et al., 2017) and  
13 regional(Li et al., 2010; Smith et al., 2010; Tang et al., 2021; Wang et al., 2020) (Wang et al., 2020; Tang  
14 et al., 2021; Zhan et al., 2014; Li et al., 2001) GHG emission studies have been conducted for a variety  
15 of agricultural sources of GHG emissions using major crops in the Chinese region, which have been well  
16 validated in China. The feasibility of the DNDC model in simulating carbon dioxide (CO<sub>2</sub>), methane  
17 (CH<sub>4</sub>), and nitrous oxide (N<sub>2</sub>O) emissions from agricultural soils is known.  
18

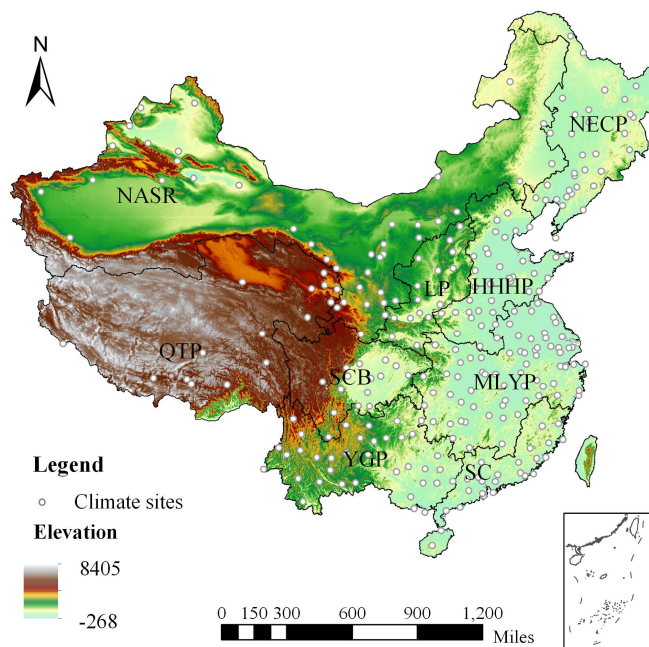
19 In this study, the DNDC model was parameterized for an actual situation in the study area. The  
20 DNDC model and Penman-Monteith formula provided by FAO (FAO-PM) were used to quantify the  
21 GHG emissions and crop water demand in 337 cities in China for six major food crops: corn, winter  
22 wheat, spring wheat, single-cropping rice, early rice, and late rice, to assess the water-carbon effect of  
23 cultivation in China. Herein, the GHG emissions and water demand in different provinces and  
24 agricultural regions were assessed; the water carbon intensity in different provinces and agricultural  
25 regions was examined; the influence of regional differences in environmental elements, especially the  
26 main meteorological elements, on the spatial distribution characteristics of agricultural water carbon  
27 intensity was determined; and a sensitivity analysis of the main factors affecting GHG emissions was  
28 conducted. The results of this study will help to assess the inter-crop and spatial heterogeneity of water-  
29 carbon fluxes, and the quantitative results can be used as evaluation indicators to establish  
30 environmentally friendly agricultural cropping patterns suitable for different cropping regions.  
31

## 32 **2. Materials and methods**

### 33 **2.1 Study area**

34 Different agricultural regions in China exhibit notable variations in climate, soil composition, and  
35 agricultural cultivation practices. To analyze the water-carbon effect and other factors at different  
36 geographical regions, China was divided into nine agricultural regions according to data from the  
37

1 Resource and Environment Science and Data Center (<https://www.resdc.cn>). These regions include  
2 Northeast China Plain (NECP), Yunnan-Guizhou Plateau (YGP), Northern arid and semiarid region  
3 (NASR), Southern China (SC), Sichuan Basin and surrounding regions (SCB), Middle-lower Yangtze  
4 Plain (MLYP), Qinghai Tibet Plateau (QT), Loess Plateau (LP), and Huang-Huai-Hai Plain (HHHP) (Fig.  
5 1). For the division, the provincial administrative region was employed as the basic unit and the  
6 geographical distribution and meteorological and agricultural production characteristics were  
7 comprehensively considered, ultimately meeting the requirements of this study.



110  
111 Fig. 1 Overview of study area (Including the division of agricultural regions, the distribution of  
112 meteorological stations and the elevation of the study area.)

## 113 2.2 Model input parameters

114 Several GIS databases were constructed to run the DNDC model (Table S1). Historical daily  
115 meteorological data (including daily maximum and minimum temperatures and precipitation) were  
116 obtained from the China Meteorological Administration (<https://data.cma.cn/>). A total of 337 basic  
117 stations in China were used from 2015 to 2016 (Fig. 1). The background CO<sub>2</sub> concentration data were  
118 the average CO<sub>2</sub> data published by the National Oceanic and Atmospheric Administration  
119 (<https://gml.noaa.gov/ccgg/trends/global.html>).

120 Soil data were obtained from the World Soil Database (HWSD) China Soil Dataset (V1.1)  
121 (<https://www.fao.org/soils-portals>). The data source in China contained 1:1 million soil data provided  
122 by the Nanjing Institute of Soil Science of the Second National Land Survey. The soil data used in this  
123 study include soil organic carbon (SOC) content, soil clay content, soil pH, and soil bulk density (Fig.  
124 S1).

125       The farmland management data were obtained from the National Bureau of Statistics of China  
126 (<https://www.stats.gov.cn/tjsj>). The data on crop planting area, irrigated area, and fertilizer application at  
127 the provincial level were collected from provincial statistical yearbooks. The crop planting area and  
128 fertilizer application rate at the municipal level were collected from the statistical yearbook of each  
129 province, the China Statistical Yearbook, and the China Rural Statistical Yearbook.

130       When calculating the evapotranspiration of crop (ET<sub>c</sub>), it is necessary to consider that different crops  
131 have different growth periods. According to the characteristics of crop growth, the growth process can  
132 be divided into four stages: early, rapid, middle, and late. The growth periods of six major crops in each  
133 province (Fig. S2) were collected according to the crop growth manual and related literature(Allen et al.,  
134 1998; Zheng, 2015).

### 135       **2.3 Global warming potential (GWP)**

136       In order to evaluate the influence of various GHGs on climate change, the global warming potential  
137 (GWP) spanning 100 years is used to express the combined warming effect of three GHGs(IPCC, 2007).  
138 It is to assess the potential climate impact of different GHGs based on their radiation properties. The  
139 calculation method is as follows:

$$140 \quad GWP = CO_2 + N_2O \times 298 + CH_4 \times 25 \quad (1)$$

141       Where *GWP* is global warming potential, kgC/ha; *CO<sub>2</sub>*is cumulative emission flux of CO<sub>2</sub>; *N<sub>2</sub>O* is  
142 cumulative emission flux of N<sub>2</sub>O; *CH<sub>4</sub>* is cumulative emission flux of CH<sub>4</sub>; 298 is the conversion factor  
143 of global warming potential between N<sub>2</sub>O and CO<sub>2</sub>; 25 is the conversion factor of global warming  
144 potential between CH<sub>4</sub> and CO<sub>2</sub>.

### 145       **2.4 Crop water demand**

146       The water calculation module embedded in the DNDC model relies on the FAO-PM formula.  
147 However, the parameter input simplifies the meteorological parameters and comprises solely three  
148 parameters: maximum temperature, minimum temperature, and maximum temperature. Therefore, in this  
149 study, the reference crop evapotranspiration (ET<sub>0</sub>) was calculated by the Penman-Monteith formula  
150 provided by FAO(Allen et al., 1998). The Penman-Monteith equation is as follows:

$$151 \quad ET_0 = \frac{0.408\Delta(R_n - G) + \gamma \frac{900}{T + 273} U_2(e_s - e_a)}{\Delta + \gamma(1 + 0.34U_2)} \quad (2)$$

152       Where *ET<sub>0</sub>* is the reference crop evapotranspiration (mm day<sup>-1</sup>); *R<sub>n</sub>* is the net radiation from the  
153 surface of the crop (MJ m<sup>-2</sup> day<sup>-1</sup>); *G* is soil heat flux (MJ m<sup>-2</sup> day<sup>-1</sup>); *T* is the air temperature at 2  
154 meters (°C); *U<sub>2</sub>* is the wind speed at 2 meters (m s<sup>-1</sup>); *e<sub>s</sub>* is the saturated vapor pressure (kPa); *e<sub>a</sub>* is

1           155 the actual water vapor pressure (kPa);  $e_s - e_a$  is the saturation vapor pressure difference (kPa);  $\Delta$  is the  
2           156 slope of the water vapor pressure curve (kPa °C<sup>-1</sup>);  $\gamma$  is the thermometer constant (kPa °C<sup>-1</sup>).  
3  
4           157  
5           158                 The  $ET_c$  was calculated according to the crop coefficient method as follows (Allen et al., 1998).  
6  
7  
8           159                 Where  $ET_c$  is the evapotranspiration of crop (mm day<sup>-1</sup>);  $K_c$  is the crop coefficient(dimensionless).  
9  
10          160                 Crop coefficients are partly influenced by meteorological conditions(Allen and Pereira, 2009). This  
11          161 study involved correcting the crop coefficients by incorporating standard values provided by the FAO  
12          162 and considering specific factors like climate, irrigation, and crop characteristics across various  
13          163 regions(Qiu et al., 2022). The correction formula for the  $K_c$  considering the effect of meteorological  
14          164 conditions is as follows:  
15  
16          165                 
$$K_c = K_{cb} + [0.04(u_2 - 2) - 0.004(RH_{min} - 45)] \left(\frac{h}{3}\right)^{0.3}$$
  
17  
18  
19  
20  
21  
22  
23  
24  
25  
26          166                 Where  $K_{cb}$  are the  $K_c$  values reported in FAO 56 for the standard climate (i.e. mean  $u_2 = 2.0$  m/s  
27  
28          167 and mean  $RH_{min} = 45\%$ ), and recently updated by (Pereira et al., 2021).;  $u_2$  is the wind speed at a  
29  
30  
31          168 height of 2m during the crop growth stage(m/s);  $RH_{min}$  is the minimum relative humidity at the crop  
32  
33  
34          169 growth stage(%);  $h$  is the average height of the crop(m).  
35  
36  
37  
38          170  
39  
40          171                 **2.5 Model validation and parameterization**  
41  
42  
43  
44  
45  
46  
47          172                 In this study, the measured data of the points in the published articles and the statistical data in the  
48  
49          173 statistical yearbook are used as the measured values to compare with the simulation results. The purpose  
50  
51          174 is to parameterize and verify the DNDC model. The validated parameters are mainly crop yields and  
52  
53          175 GHG emission fluxes.  
54  
55  
56          176                 In this study, the Monte Carlo method was used to parameterize the model and perform sensitivity  
57  
58          177 analysis. The parameterization process is as follows:  
59  
60  
61          178                 step1: To establish the parameter variation range, references were consulted, encompassing values  
62  
63          179 previously documented in the literature. This range was then extended by 20% to encompass a wider  
64  
65          180 spectrum of values, ensuring a comprehensive set of options for subsequent parameter tuning.  
66  
67  
68          181                 step2: The parameter gradient change step was determined based on the anticipated number of  
69  
70          182 simulations and the range of parameter changes.  
71  
72  
73          183                 Step3: Combination of three parameters for simulation.

184 Step4: The parameterization result is determined by selecting the set of parameter values that  
185 closely match the statistical value obtained from the run result, with the yield serving as the target value.  
186

Step5: If the error in the simulation result exceeds 30%, proceed to step 2.

187 Root mean square error (RMSE) and Pearson correlation coefficient ( $R^2$ ) were used to evaluate the  
188 correlation between the measured and simulated values.

$$RMSE = \sqrt{\frac{\sum_{i=1}^n (O_i - S_i)^2}{n}} \quad (5)$$

Where  $O_i$  is the observed value;  $S_i$  is the simulated value.

$$R^2 = \frac{SSR}{SST} = \frac{\sum (\hat{y}_i - \bar{y})^2}{\sum (y_i - \bar{y})^2} \quad (6)$$

$\hat{y}_i$  is the simulated value;  $y_i$  is the observed value;  $\bar{y}$  is the average of the observed value.

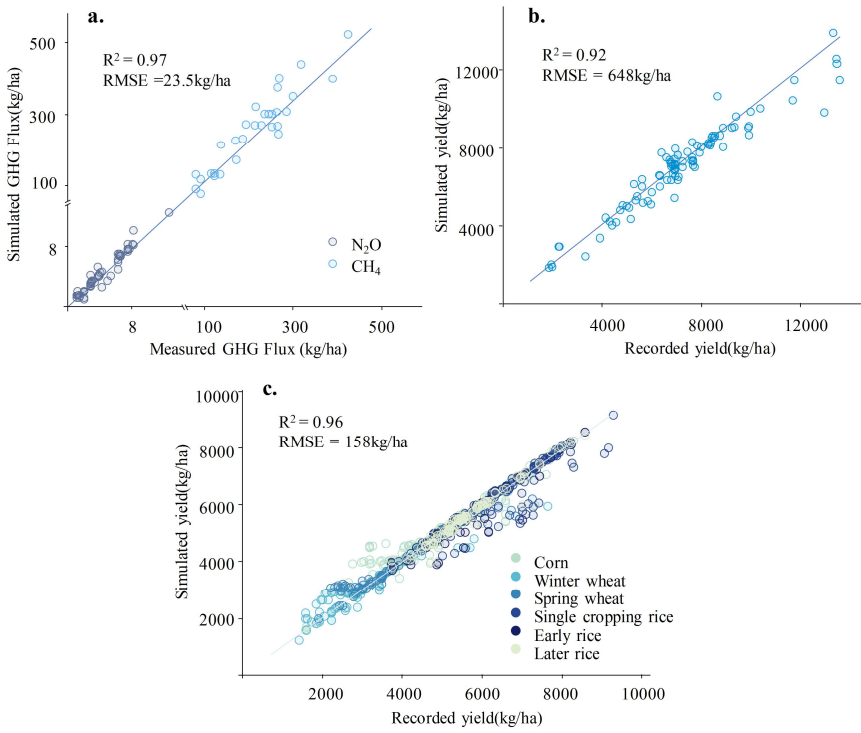
### 3. Results

#### 3.1 Model validation and parameterization

We collected point-site experimental data for various regions in China from previous studies to verify the adaptability of the DNDC model in the study area, including production and gas emission flux. Based on point validation, the experimental data of rice, wheat, and corn were collected from previously published literature, including 95 sets of yield data (Table S3). There were 30 groups of CH<sub>4</sub> emission flux data and 54 groups of N<sub>2</sub>O emission flux data. The verification results are shown in Fig. 2a.

The  $R^2$  of the observed and simulated values of the GHG emission fluxes was 0.97, and the RMSE was 23.5 kg/ha. The  $R^2$  of the observed and simulated yield values was 0.92, and the RMSE was 648 kg/ha. The simulation results of DNDC matched well with the observed results, indicating that the DNDC model has good adaptability within the scope of China.

The simulated yield of the DNDC model was compared with the recorded yield in the statistical yearbook as a validation factor (Fig. 2b), and a total of 1,191 simulated sample points were obtained for six types of crops. Using the Monte Carlo method, the main input parameters, including the maximum biomass, growth period, water demand, and other factors were matched regionally. After parameterization, the simulation results of the model matched most provinces and cities in China. The fitted  $R^2$  value of the simulated and observed yield was 0.96 (n=1191), and the RMSE was 158 kg/ha. All crop yield simulation models performed well.



211  
212 Fig. 2 Point and region verification results (a. comparison between modeled and observed GHG flux at  
213 point sites, b. comparison between modeled and observed yield flux at point sites,c. Regional  
214 comparison of simulated and recorded yields)

215 In this study, the DNDC model was parameterized using yield as the validation objective. The  
216 parameterization mainly focused on three crop parameters: Max grain yield, Ratio of grain organs, and  
217 TDD. The municipal scale was used for these crop parameters. The range of variation for these  
218 parameters across 337 municipal regions in China is presented in Table 1.

219 Table 1 Parameterized range of major crop parameters

Crop	Variables	Database
Corn	Max grain yield (kgC/ha)	2000-5000
	Ratio of grain organs	0.25-0.4
	TDD ( $^{\circ}\text{C}$ )	1800-2100
Wheat	Max grain yield (kgC/ha)	500-2500
	Ratio of grain organs	0.25-0.45
	TDD ( $^{\circ}\text{C}$ )	1600-1900
Rice	Max grain yield (kgC/ha)	2000-5000
	Ratio of grain organs	0.2-0.4
	TDD ( $^{\circ}\text{C}$ )	1900-2200

220 Note: Crop parameters for winter and spring wheat varied across simulation units, although the range of  
221 variation remained consistent. Similarly, this held true for early, late, and single-season rice.  
222

### 223 3.2 Assessment of GHG emissions and water demand in China

224           **3.2.1 Overview of GHG emissions and water demand in China**

225       In this study, the emissions of CO<sub>2</sub>, CH<sub>4</sub>, and N<sub>2</sub>O in farmland soil and the water demand during  
226       the growth period of six types of crops (corn, winter wheat, spring wheat, single-cropping rice, early rice,  
227       and late rice) in China were simulated. The total CO<sub>2</sub> emission was 372.43 Tg/yr, the total CH<sub>4</sub> emission  
228       was 11.68 Tg/yr, the total N<sub>2</sub>O emission was 475.56 Gg/yr; and the total water demand was 473.60 Gm<sup>3</sup>.  
229       The emissions and water demand of each crop are shown in Table 2.

230           **Table 2 Total GHG emissions from various crops in China**

	CO <sub>2</sub> (Tg/yr)	CH <sub>4</sub> (Tg/yr)	N <sub>2</sub> O (Gg/yr)	Water demand (Gm <sup>3</sup> )
Corn	128.80	\	205.60	181.57
Winter wheat	90.21	\	103.80	85.46
Spring wheat	4.34	\	4.58	7.22
Single-cropping rice	104.77	8.39	50.44	146.62
Early rice	41.92	1.46	45.51	21.94
Late rice	43.20	2.11	63.28	30.80
Total	413.24	11.97	473.20	473.60

231       Corn was the main source of CO<sub>2</sub> emissions from farmlands in China, accounting for 35% (128.87  
232       Tg/yr) of the total CO<sub>2</sub> emissions. Single-cropping rice had a high CH<sub>4</sub> emission, accounting for 72%  
233       (8.44 Tg/yr) of the total CH<sub>4</sub> emissions. Similar to the emission trend of CO<sub>2</sub>, N<sub>2</sub>O emissions of corn  
234       were largest, accounting for 43% (205.85 Gg/yr) of the total N<sub>2</sub>O emissions. Differences in planting area  
235       and emission intensity were the main reasons for the differences in emissions between crops.

236       During the study period, the total water demand of the major grain crops in China was 473.60 Gm<sup>3</sup>,  
237       and the national average ET<sub>c</sub> was 424.14 mm. Affected by planting area, the water demand of corn was  
238       181.57 Gm<sup>3</sup>, accounting for 38% of the total water demand.

239       Owing to many factors such as climatic conditions and policies, the distribution of crops in China  
240       had obvious differences among administrative regions. In this study, the planting area, planting structure,  
241       GHG emissions, and water demand of each province were compared to explore the differences in  
242       agricultural water and carbon among the provinces and their corresponding relationships with crops (Fig.  
243       3).

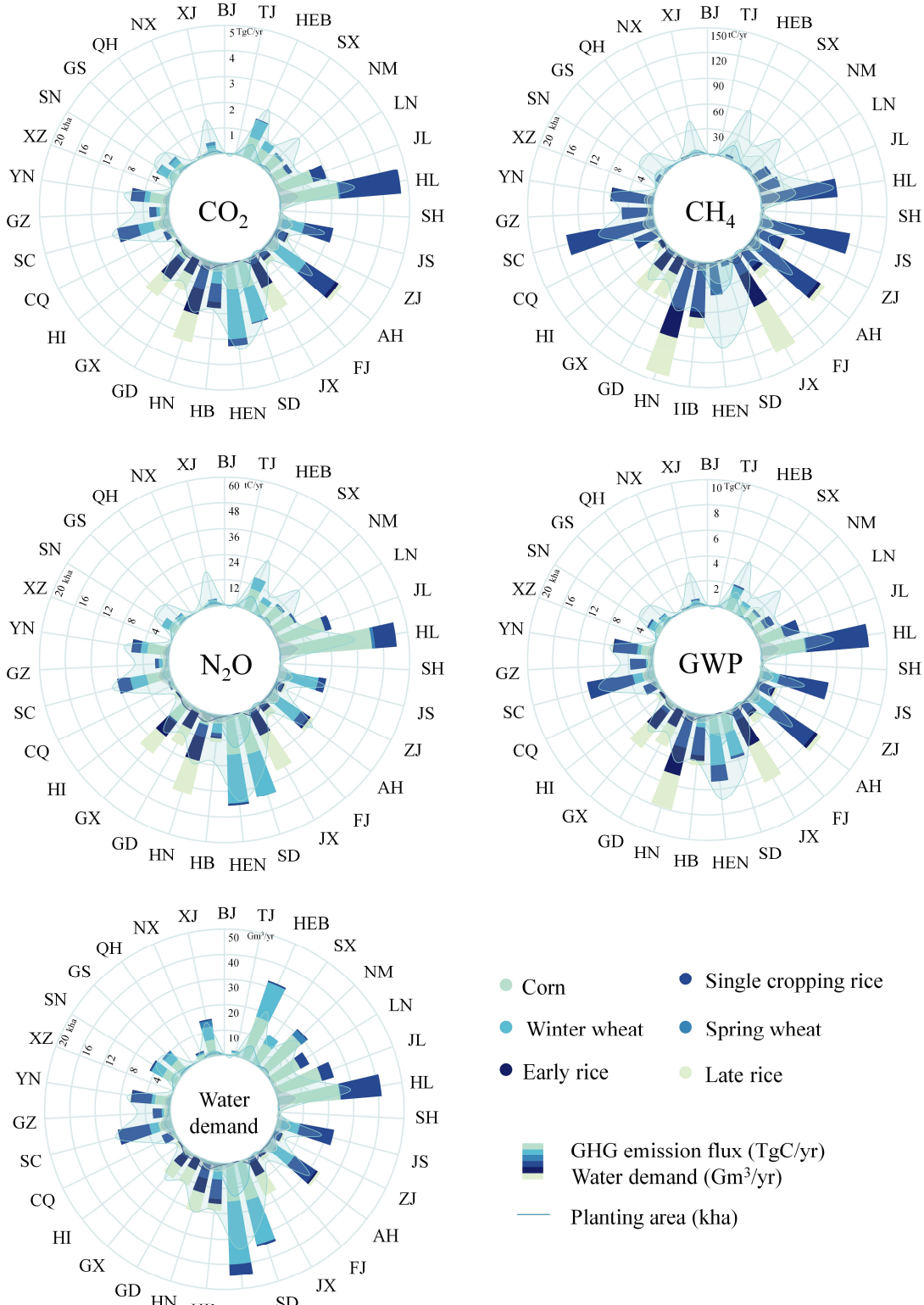


Fig. 3 Radar map of provincial GHG emissions, crop water demand and planting area(Stacked bars show the total GHG emissions of different crops, the radar chart shows the acreage of various crops; Use different colors to distinguish crops; the provinces represented by the English abbreviations were shown in Table S4)

### 3.2.2 Spatial distribution characteristics of GHG emissions from major grain

244

245

246  
247  
248  
249

250

251

252

253

254

255

256

257

258

259

260

261

262

263

264

265

266

267

268

269

270

271

272

273

274

275

276

277

278

279

280

281

282

283

284

285

286

287

288

289

290

291

292

293

294

295

296

297

298

299

300

301

302

303

304

305

306

307

308

309

310

311

312

313

314

315

316

317

318

319

320

321

322

323

324

325

326

327

328

329

330

331

332

333

334

335

336

337

338

339

340

341

342

343

344

345

346

347

348

349

350

351

352

353

354

355

356

357

358

359

360

361

362

363

364

365

366

367

368

369

370

371

372

373

374

375

376

377

378

379

380

381

382

383

384

385

386

387

388

389

390

391

392

393

394

395

396

397

398

399

400

401

402

403

404

405

406

407

408

409

410

411

412

413

414

415

416

417

418

419

420

421

422

423

424

425

426

427

428

429

430

431

432

433

434

435

436

437

438

439

440

441

442

443

444

445

446

447

448

449

450

451

452

453

454

455

456

457

458

459

460

461

462

463

464

465

466

467

468

469

470

471

472

473

474

475

476

477

478

479

480

481

482

483

484

485

486

487

488

489

490

491

492

493

494

495

496

497

498

499

500

501

502

503

504

505

506

507

508

509

510

511

512

513

514

515

516

517

518

519

520

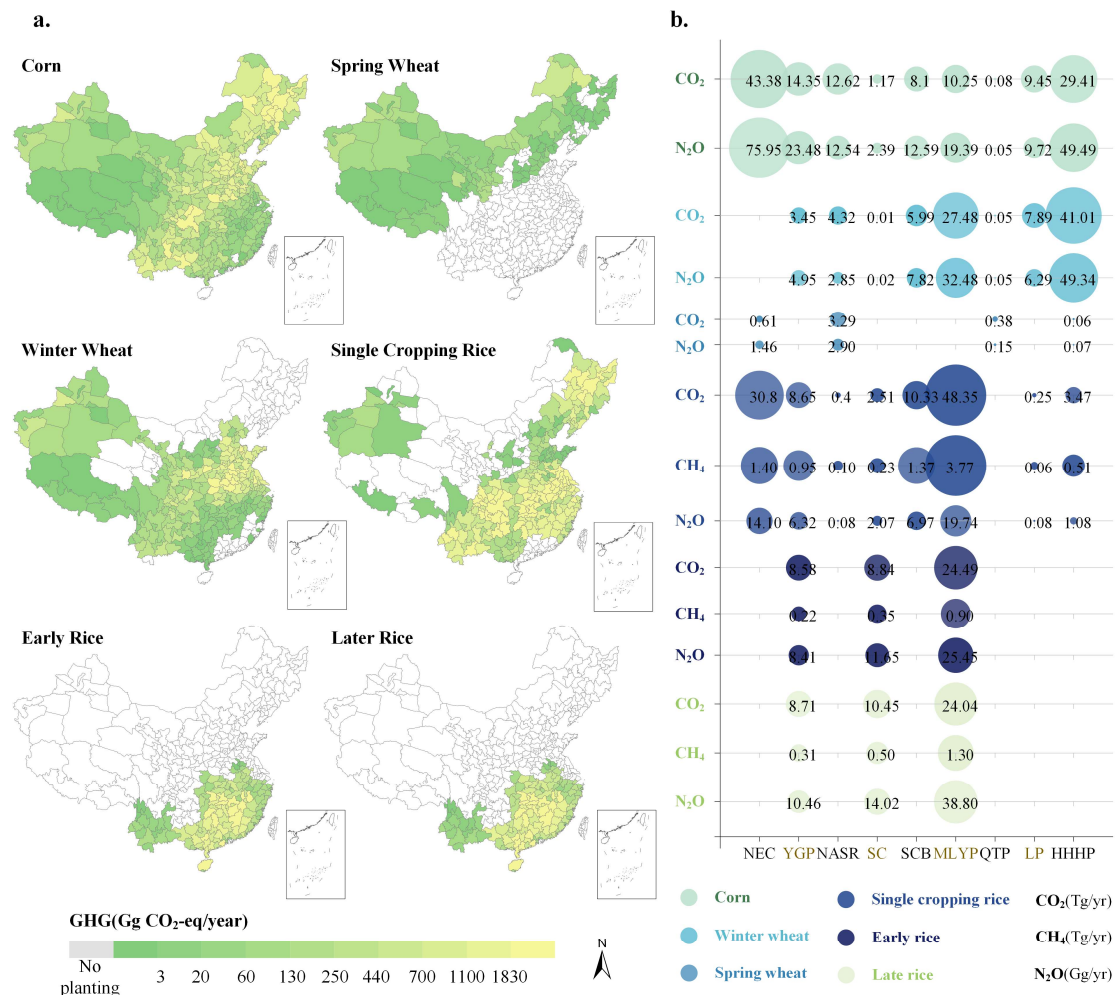
521

522

523

250 The spatial distributions of total CO<sub>2</sub>, CH<sub>4</sub>, N<sub>2</sub>O emissions and GWP of the six types of major food  
 251 crops at the municipal scale are shown in Fig. 4a and Fig. S3-S5, respectively. As corn, winter wheat,  
 252 and spring wheat are dry land crops and not CH<sub>4</sub> sources, only CO<sub>2</sub> and N<sub>2</sub>O emissions were assessed.  
 253 The CO<sub>2</sub>, CH<sub>4</sub>, and N<sub>2</sub>O emissions from single-cropping rice, early rice, and late rice were evaluated.  
 254

255 Significant differences were found in the spatial distribution of GHG emission hotspots for different  
 256 crops. Corns are widely distributed across various provinces and cities in China. The provinces that  
 257 mainly cultivated corn formed a corn planting strip from the northeast to southwest, and the corn planting  
 258 area in these provinces was more than 1 Mha. The cities with large municipal GHG emissions were  
 259 concentrated in northeast China, and the CO<sub>2</sub> emission of corn in this region was 43.38 Tg/yr, accounting  
 260 for 34% of the total national emission. The total emission of N<sub>2</sub>O was 75.95 Gg/yr, accounting for 37%  
 261 of the total emissions.



262  
 263 Fig. 4 Annual GHG emissions (a.total GHG equivalent emissions of each crop; b. bubble chart of GHG  
 264 emissions from nine agricultural regions in China)

265 Owing to climate and production conditions, only some provinces and cities in northeast, south, and

1       266 northwest China do not cultivate winter wheat. Winter wheat contributes significantly to GHG emissions  
2       267 owing to its long growth period. In terms of spatial distribution, the hotspots of winter wheat emissions  
3       268 were mainly concentrated in HEB, SX, JS, AH, SD, HEN, SN, and SC (Fig. 4b). The HHHP is the hotspot  
4       269 of CO<sub>2</sub> emissions from winter wheat, and the total CO<sub>2</sub> emission in this region was 41.01 Tg/yr,  
5       270 accounting for 45% of the total CO<sub>2</sub> emissions. The total N<sub>2</sub>O emission in this region was 49.34 Gg/yr,  
6       271 accounting for 48%.

7       272 Spring wheat is generally cultivated in regions without winter wheat planting conditions, and the  
8       273 accumulated temperature during the growth period is the main standard. Therefore, the provinces in  
9       274 northern China and Tibet in southwest China, which have high latitudes and low temperatures, are the  
10      275 main planting areas for spring wheat in China. Owing to its smaller acreage, spring wheat has  
11      276 significantly lower GHG emissions than other crops. In terms of geographical distribution, the higher the  
12      277 latitude of the city, the greater is its GHG emissions from spring wheat. The hottest spots of spring wheat  
13      278 GHG emission were concentrated in NASR, and the total CO<sub>2</sub> emission in this region was 3.29 Tg/yr,  
14      279 accounting for 76% of the total CO<sub>2</sub> emission in China. The total N<sub>2</sub>O emission in this region was 2.9  
15      280 Gg/yr, accounting for 63% of the national total.

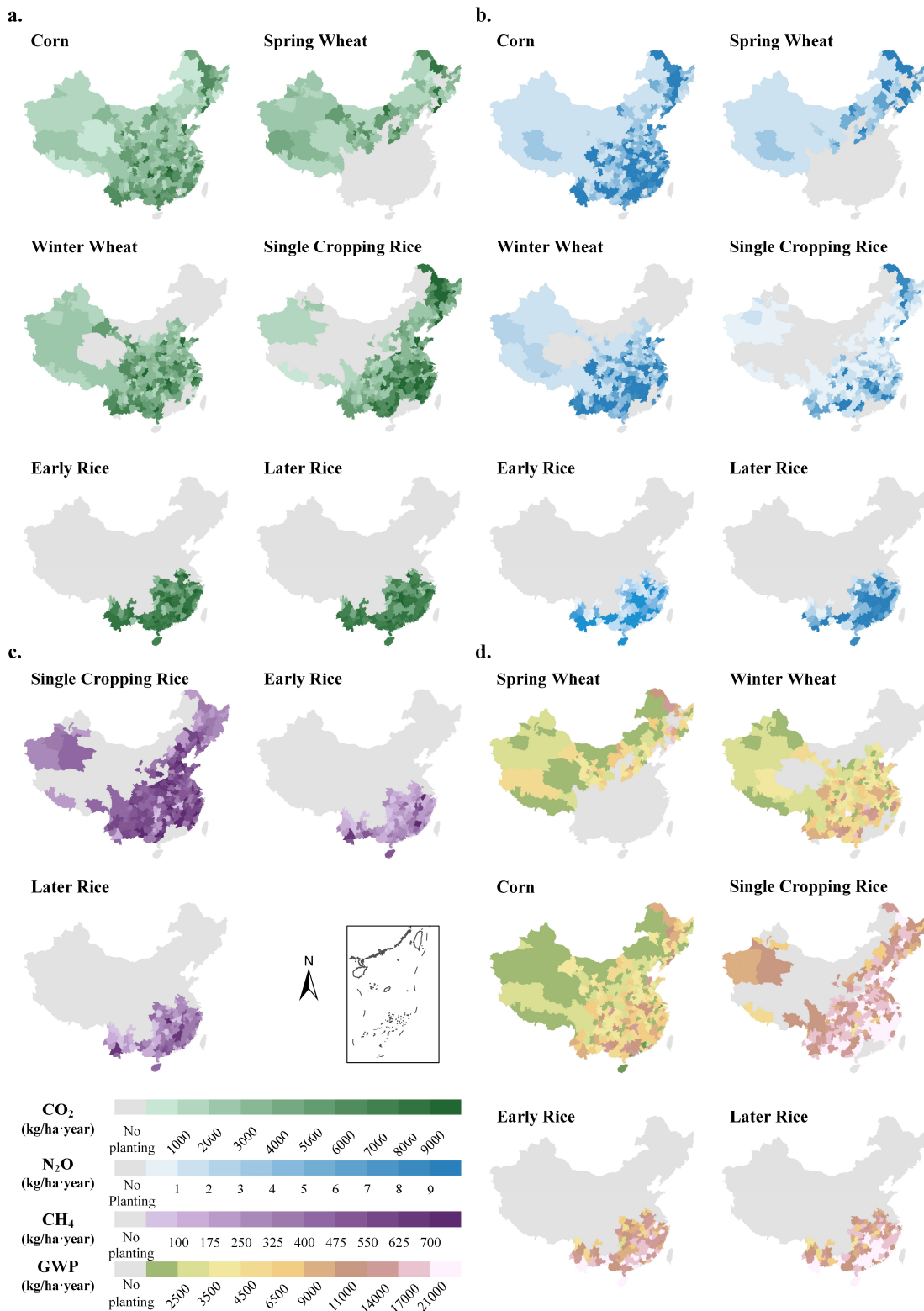
16      281 Except for the NASR, QT, some unsuitable areas in LP, and the areas more suitable for double-  
17      282 cropping rice in SC, single-cropping rice was cultivated in all other regions. MLYP and NECP were the  
18      283 two hotspots of CO<sub>2</sub> emission from single-cropping rice. The total CO<sub>2</sub> emission in the MLYP was 48.35  
19      284 Tg/yr, accounting for 46% of the national total. The total N<sub>2</sub>O emission was 19.74 Gg/yr, accounting for  
20      285 39% of the total national emissions. The total CO<sub>2</sub> emission in NECP was 30.80 Tg/yr, accounting for  
21      286 29% of the national total. The total N<sub>2</sub>O emission was 14.10 Gg/yr, accounting for 28% of the national  
22      287 total.

23      288 Early and late rice have high requirements for accumulated temperature during the growing period  
24      289 and are mainly distributed in southern China due to geographical conditions. The planting areas of early  
25      290 rice and late rice had a high degree of coincidence, and the hot spots of early rice emissions were  
26      291 relatively consistent. MLYP, SC, and YGP were the most suitable areas for rice growth. Similar to single-  
27      292 cropping rice, both early and late rice had large planting areas, they were also sources of high amounts  
28      293 of emissions in the MLYP. In this region, the total CO<sub>2</sub> emissions of early rice and late rice were 24.49  
29      294 Tg/yr and 24.04 Tg/yr, accounting for 58% and 56% of the total CO<sub>2</sub> emissions, respectively. The N<sub>2</sub>O  
30      295 emissions of early rice and late rice in this region were 25.45 Gg/yr and 38.80 Gg/yr, accounting for 56%  
31      296 and 61% of the total emissions, respectively. The CH<sub>4</sub> emissions of early rice and late rice in this region  
32      297 were 0.90 Tg/yr and 1.30 Tg/yr, respectively, both accounting for 61% of their respective total emissions  
33      298 at the national level.

1            We considered the combined contribution of the six types of crops to GHG emissions. The MLYP  
2        had the largest CO<sub>2</sub>, CH<sub>4</sub> and N<sub>2</sub>O emissions, with values of 134.61 Tg/yr, 5.94 Tg/yr, and 135.86 Gg/yr,  
3        respectively, accounting for 33%, 51%, and 29% of the total national emissions, far exceeding those of  
4        other regions.  
5  
6

7            Owing to differences in climatic conditions, soil properties, and field management practices, there  
8        are significant spatial differences in the intensity of GHG emissions from major crops in China. The three  
9        main agricultural sources of GHG emission intensity of CO<sub>2</sub>, CH<sub>4</sub>, and N<sub>2</sub>O have an overall consistency  
10      in spatial distribution. The regions with high emission intensity were mainly distributed in NECP, MLYP,  
11      YGP, and SC. The overall Thiel coefficients (T) for CO<sub>2</sub>, CH<sub>4</sub>, and N<sub>2</sub>O emissions in China were 0.04,  
12      0.22, and 0.13, respectively, indicating that CH<sub>4</sub> has the largest spatial variation among the three GHGs.  
13  
14

15           Significant differences were found in the emission intensities of different crops, and the CO<sub>2</sub>  
16        emission intensity of early rice was the highest (7,365 kg/ha). The average growth period of single-  
17        cropping rice was 140 days, which was longer than that of early (119 days) and late (133 days) rice.  
18           Moreover, the emission intensity of CH<sub>4</sub> from single-cropping rice was the highest. The difference in  
19        CO<sub>2</sub> emission intensity caused by the different crop types was smaller than that caused by the external  
20        environment. The spatial distribution of the CO<sub>2</sub> emission intensity of major food crops is shown in Fig.  
21        5a. Horizontal comparison revealed that the CO<sub>2</sub> emission intensity of rice crops was generally higher  
22        than that of drought crops. The emission intensity of CH<sub>4</sub> was significantly different between dryland  
23        and aquatic crops. CH<sub>4</sub> is only emitted by rice crops and is related to the growth of crops. The spatial  
24        distribution of the CH<sub>4</sub> emission intensity of rice crops is shown in Fig. 5c.  
25  
26  
27  
28  
29  
30  
31  
32  
33  
34  
35  
36  
37  
38  
39  
40  
41  
42  
43  
44  
45  
46  
47  
48  
49  
50  
51  
52  
53  
54  
55  
56  
57  
58  
59  
60  
61  
62  
63  
64  
65



319  
320      Fig. 5 emission intensity of major crops (a.CO<sub>2</sub>; b.N<sub>2</sub>O; c.CH<sub>4</sub>;d.GWP)

321      Considering the overall effects of the three GHGs, the municipal level GWP of five major food  
322      crops in China was analyzed, and the spatial distribution is shown in Fig. 5d. By comparing the total  
323      emissions of the six types of crops, the GWP of rice crops was found to be generally greater than those

1       324 of corn, spring wheat, and winter wheat; this is mainly because rice crops are not only the main source  
2       325 of CO<sub>2</sub> and N<sub>2</sub>O emissions, but also the source of CH<sub>4</sub> emissions. Compared with early rice, the GWP  
3       326 of single-cropping rice and late rice was almost the same, with a national average GWP of 18,251.09  
4       327 kg/ha and 18,613.55 kg/ha, respectively.

5       328 GHG emission intensities exhibited spatially distributed differences in different agricultural regions.  
6       329 The CO<sub>2</sub> and N<sub>2</sub>O emission intensity and GWP of spring wheat were the highest in NECP, with 7,863  
7       330 kg/ha, 18.97 kg/ha, and 13,346.11 kg/ha, respectively. The regions with the highest CO<sub>2</sub> emission  
8       331 intensity for early and late rice and the highest N<sub>2</sub>O emission intensity for late rice were YGP, with 9,154  
9       332 kg/ha, 8,831 kg/ha, and 10.61 kg/ha, respectively. The highest intensity of CO<sub>2</sub> emissions from corn and  
10      333 single-cropping rice, the highest intensity of CH<sub>4</sub> emissions from early and late rice, and the highest  
11      334 intensity of N<sub>2</sub>O emissions from corn, winter wheat, single-cropping rice, and early rice were found in  
12      335 SC. The SCB had the highest CO<sub>2</sub> emission intensity for winter wheat (5,042 kg/ha). Considering the  
13      336 joint contribution of six major food crops, the emission intensity of CO<sub>2</sub> and N<sub>2</sub>O as well as GWP were  
14      337 the highest in South China, with 7,162.76 kg/ha, 9.39 kg/ha, and 17816.59 kg/ha, respectively (Fig. 8a-  
15      338 d). The national average emission intensity of single-cropping rice was 464 kg/ha, which is markedly  
16      339 higher than that of early and late rice owing to its longer reproductive period. The regions with the highest  
17      340 CH<sub>4</sub> emission intensity were the HHHP, where only single-cropping rice was grown (590 kg/ha).

### 342     **3.2.3 Spatial distribution characteristics of water demand from major grain**

343     The difference in meteorological conditions was the main reason for the differences in crop water  
344     demand in different regions, while the difference in the crop growth period was the main reason for the  
345     difference in water demand between crops. In this study, crop water demand were estimated at the  
346     municipal level for six major crops (Fig. 6). Significant differences were found in the crop water demand  
347     between regions and crops.

348     The ET<sub>c</sub> rankings for the six major food crops were single-cropping rice, late rice, spring wheat,  
349     corn, winter wheat, and early rice. The water demand of late rice was significantly higher than that of  
350     several other crops in all cities, with the highest average ET<sub>c</sub> of 530.95 mm. The lowest mean ET<sub>c</sub> for  
351     winter wheat was 378.95 mm. Differences in crop will directly determine the crop growth period, crop  
352     coefficients, and thus the ET<sub>c</sub> differences between crops.

353     The magnitude of regional crop water demand is mainly influenced by the spatial heterogeneity of  
354     meteorological elements, crop cultivation types, and planted areas in different regions. NASR had the  
355     highest ET<sub>c</sub> for corn and single-cropping rice, with 518.02 mm and 791.31 mm, respectively. QTP had  
356     the highest ET<sub>c</sub> for winter wheat and spring wheat, with 591.96 mm and 490.05 mm, respectively. The

357 SC for the regions with the highest  $ET_c$  for early rice and late rice was 469.45 mm and 604.61 mm,  
358 respectively.

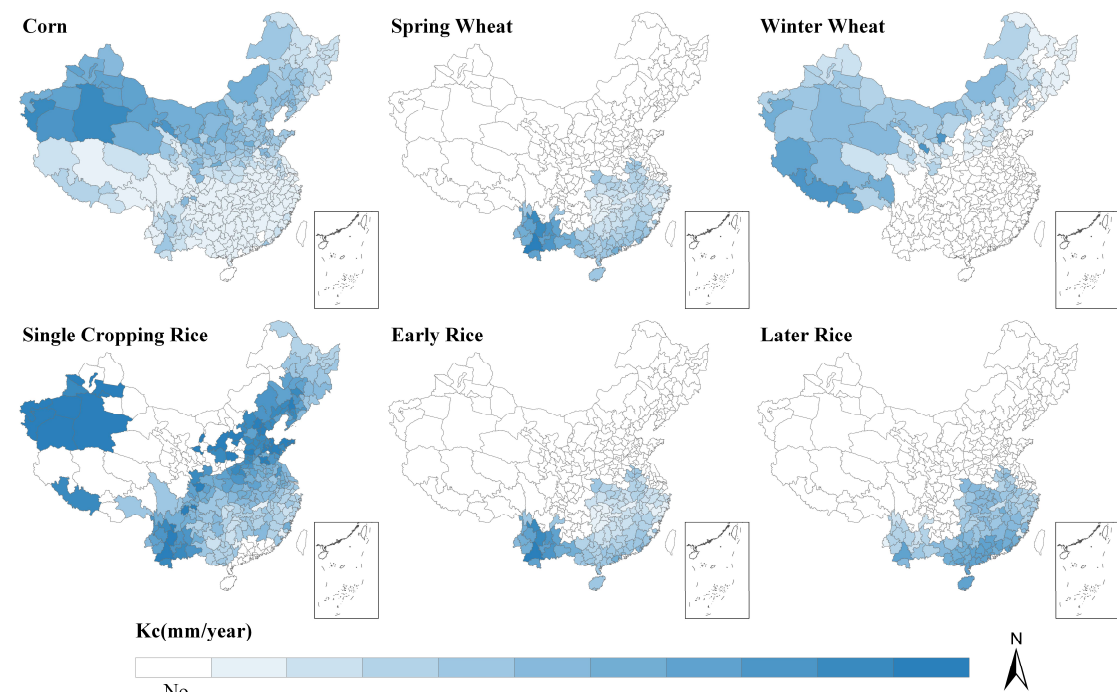


Fig. 6  $ET_c$  of major crops

360  
361 As shown in fig.6, the geospatial distribution of GHGs and water demand displayed opposite  
362 patterns. The emission intensity and GWP distribution trends of the three major GHGs were relatively  
363 consistent, and were high in Southeast China and low in Northwest China. The distribution trend of  $ET_c$   
364 was the opposite, with a high water demand concentrated in the northwest.  
365

### 366 3.3 Impact of regional climate diversity on GHG emissions and the water demand of cropland.

367 To consider the combined effects of regional climate change on the water-carbon effect on cropland,  
368 two factors of 337 cities in China in 2015, precipitation and temperature, which have significant effects  
369 on both GHG emissions and crop water demand, were selected to analyze the differences among different  
370 climate regions (Fig. 7). The national average temperature was 14.27 °C and the annual precipitation was  
371 988.24 mm in 2015. The distribution of temperature and precipitation in China varied significantly  
372 among agricultural regions. In fact, the high-temperature region had a spatial distribution consistent with  
373 the high-precipitation region. SC had the highest annual precipitation and average annual temperature,  
374 with an annual precipitation of 1,743 mm and an average annual temperature of 21.85 °C. The regional  
375 distribution of the lowest annual precipitation and mean annual temperature was not consistent. NASR  
376 had the lowest annual precipitation, which was only 15.1% of that in the SC. QT had the lowest annual  
377 average temperature, which is 23.9% of that in SC. According to Fig. 7Fig. 8 and Fig. 8, the spatial

1 distributions of precipitation and crop water demand were reversed. Crop water demand were small in  
2 areas with high precipitation as differences in the wetness of farmland would affect crop water demand(F.  
3 Yan et al., 2021). The NASR had the lowest annual precipitation, which was only 15.1% (264 mm) of  
4 that of southern China. In contrast, this region had the highest ET<sub>c</sub> (525.91 mm).

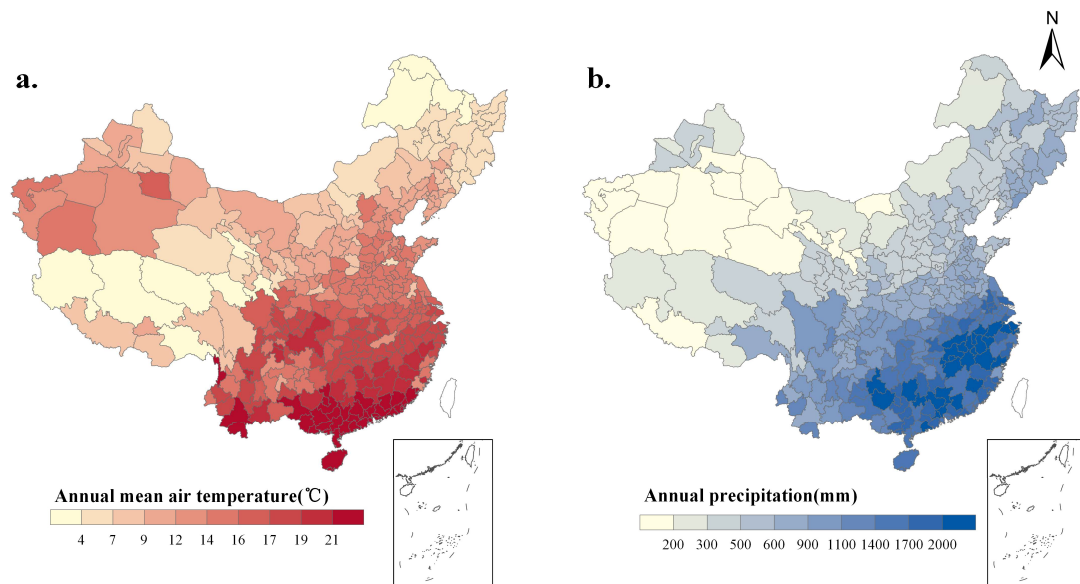


Fig. 7 Annual precipitation and average temperature

On one hand, the development of crops was stimulated, the number of leaves was increased, and leaf area index was increased. An increase in the leaf area index would increase the transpiration and water demand of crops. An increase in LAI would increase soil cover and reduce soil surface temperature and soil evaporation, thereby reducing water demand. However, an increase in temperature accelerates the growth and development of crops, resulting in a shorter crop reproductive period, which in turn reduces crop water demand (Han et al., 2017; Jia et al., 2019; Saadi et al., 2015). In this study, a uniform fertility period was established for the crop in each province; therefore, this influence factor was not significant within the province.

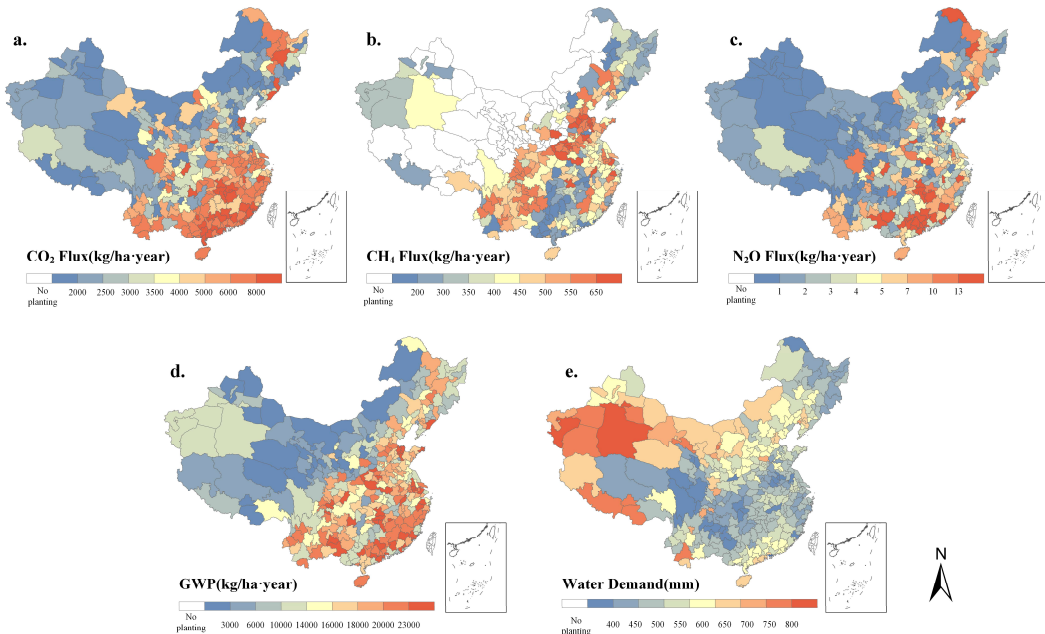


Fig. 8 GHG emission intensity and crop water demand

The hotspot areas of GHG emissions were consistent in spatial distribution with high-temperature and high-precipitation areas. Not all regions with the highest crop emissions had the highest annual precipitation and average temperature due to differences in emission characteristics among crops. The higher the temperature, the greater is the respiration intensity of the soil, which includes soil microbial respiration, soil animal respiration, root respiration, and chemical oxidation processes that promote the emission of soil GHGs (Koponen et al., 2006; Lu et al., 2022; Niraula et al., 2018). Within a certain range, the increase in temperature accelerates the decomposition of soil organic matter while stimulating the activity of soil methanogens and providing favorable conditions for soil CH<sub>4</sub> emission (Wang et al., 1997). Chemical fertilizers are commonly applied to Chinese farmlands, and studies have shown that an increase in temperature accelerates the release of N fertilizers, ultimately increasing N emissions from the soil (Shcherbak et al., 2014; Smith, 2017).

Precipitation processes would usually result in a rapid increase in soil moisture and changes in soil physical and chemical properties, such as soil permeability and organic matter concentration in the soil solution. Further, the root systems of different plants respond differently to these changes. Precipitation has polarized effects on GHG emissions in different climatic zones. Studies have shown that for wetter areas, precipitation inhibits soil respiration, whereas in drier or alternating wet and dry areas, precipitation stimulates soil respiration, causing more GHG emissions (J. Yang et al., 2022; Zhang et al., 2021), which is consistent with the results of this study.

1           **4. Discussion**

2           **4.1 Sensitivity analysis**

3  
4           Based on previous studies, seven factors that had a significant impact on GHG emissions were  
5           selected for sensitivity analysis, including soil capacity, soil organic carbon content, soil clay content,  
6           soil pH, air temperature, precipitation, and nitrogen fertilizer use (Fig. 9).

7  
8           Based on the simulation results, differences were found in the sensitivities of different crops to  
9           parameter changes. Soil is a source of GHG emissions from agriculture, and differences in soil properties  
10          would have a decisive impact on the intensity and type of GHG emissions. Differences in the variation  
11          of soil parameters produced by different crops are particularly pronounced. Changes in meteorological  
12          elements are indirectly induced relative to the effect of changes in soil elements on GHG emissions, such  
13          as changes in temperature that act on the soil to affect soil temperature and precipitation, ultimately  
14          changing the soil water content. Similarly, changes in meteorological elements would induce different  
15          response efficiencies among crops.

16  
17          An increase in soil bulk density decreases soil porosity, which reduces the oxygen content of the  
18          soil and thus inhibits soil GHG emissions (Novara et al., 2012; P. Yang et al., 2022). The CO<sub>2</sub> emission  
19          intensity of corn, CH<sub>4</sub> emission intensity of late rice, and N<sub>2</sub>O emission intensity of winter wheat were  
20          found to be more sensitive to changes in soil capacitance. In contrast, the CO<sub>2</sub> emission intensity of  
21          winter wheat, CH<sub>4</sub> emission intensity of late rice, and N<sub>2</sub>O emission intensity of single-cropping rice  
22          were more sensitive to changes in clay.

23  
24          SOC is an important substrate for GHG emissions and the dominant factor controlling soil GHG  
25          emissions (Ye et al., 2016). The CO<sub>2</sub> emission intensity of spring wheat, CH<sub>4</sub> emission intensity of late  
26          rice, and N<sub>2</sub>O emission intensity of winter wheat were sensitive to changes in SOC.

27  
28          An increase in air temperature has an impact on soil temperature, which in turn affects the intensity  
29          of biochemical reactions in the soil and increases the intensity of GHG emissions (Koponen et al., 2006;  
30          Lu et al., 2022; Wang et al., 1997). The CO<sub>2</sub> emission intensity of corn, CH<sub>4</sub> emission intensity of early  
31          rice, and N<sub>2</sub>O emission intensity of single-cropping rice were more sensitive to temperature changes.

32  
33          An uncertainty exists regarding the effect of precipitation on emissions. The intensity of emissions  
34          is related to the intensity of a single precipitation event and the amount of precipitation (J. Yang et al.,  
35          2022; Zhang et al., 2021). Our evaluation of precipitation in the sensitivity analysis aimed to increase or  
36          decrease the actual daily precipitation by a corresponding gradient on a daily scale. Fluctuations in  
37          precipitation at the daily scale can increase the uncertainty of the study, such as accumulating a larger  
38          amount of precipitation at one time, thereby exceeding the moisture threshold for soil emissions and  
39          reducing soil emissions; or increasing the water content of the soil within a certain range, thereby

promoting soil GHG emissions. The CO<sub>2</sub> emission intensities of spring wheat and late rice and N<sub>2</sub>O emission intensity of spring wheat were more sensitive to changes in precipitation.

Increases in N fertilizer inputs would significantly stimulate GHG emissions from farmland, particularly CH<sub>4</sub> and N<sub>2</sub>O emissions. The appropriate amount of fertilizer application would provide basic N elements for crop growth and enhance microbial activity, soil structure, soil permeability, and emission performance. The CO<sub>2</sub> emission intensity of winter wheat, CH<sub>4</sub> emission intensity of single-cropping rice, and N<sub>2</sub>O emission intensity were more sensitive to changes in N fertilizer input.

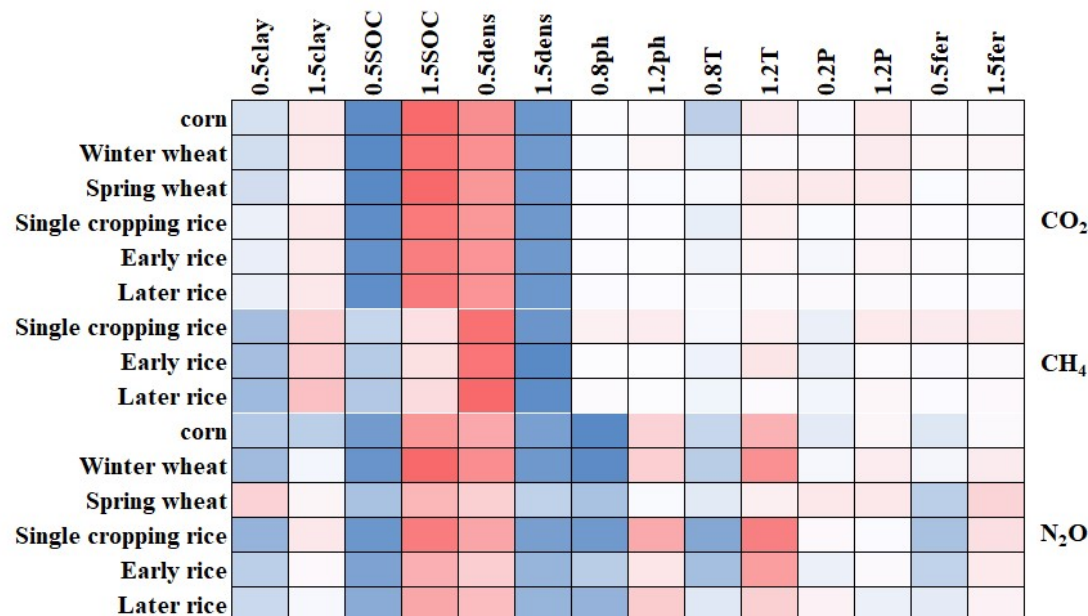


Fig. 9 Sensitivity Analysis Heat Map(the corresponding gradients of variation were set according to the range of different parameters to determine the effects of changes in these factors on GHG emissions from the agricultural fields of major crops)

#### 4.1 Water saving and emission reduction in agriculture

Based on the above studies, the water carbon effect of farmland mainly varies among crops and regions. By comparing the water-carbon effect of six types of crops, the emission intensity and water demand of rice crops were found to be markedly higher than those of dry crops, mainly because rice was the main source of CH<sub>4</sub>. The emission intensity of late rice in the double-season rice was higher than that in the early season rice. During water demand and agricultural planning, the differences in the water-carbon effects of different crops must be fully considered and the planting structure must be adjusted on this basis to ultimately achieve water conservation and emission reduction in agriculture.

By comparing the water-carbon effects of nine agricultural regions in China, the emission intensity of southern agricultural regions markedly greater than that of the northern agricultural regions. The  $ET_c$  and emission intensity displayed opposite trends in other agricultural regions, except for SC, where both

1           the water and carbon effects were high. Food production can shift from areas with high water  
2           consumption and high emissions to areas with low water consumption and low emissions, and more food  
3           can be produced with less water and lower emissions to relieve water pressure and promote sustainable  
4           agricultural development. The efficiency of response to environmental changes varies among crops.  
5  
6           Overall, soil improvement, reasonable adjustment of nitrogen application, and targeted fertilization  
7           programs can be carried out for different regions and crops to help mitigate the impact of farmland  
8           emissions on the greenhouse effect.  
9  
10

#### 11           **4.2 Uncertainty and limitations**

12           The uncertainty in the simulation results of this study focuses on three main aspects. Firstly, there  
13           was uncertainty in the input data. Although all data input to the model was obtained from official Chinese  
14           statistics or statistics from world authorities to ensure accuracy, there was still uncertainty in crop yields,  
15           climatic conditions, and soil properties. Soil properties were particularly sensitive factors (Zhang et al.,  
16           2010). In this study, the soil data used in the model is from the HWSD. However, due to tillage, soil  
17           organic carbon content might continue to decline, leading to a possible overestimation of GHG emissions.

18           Secondly, there is uncertainty in the model itself. Previous studies had shown that the model  
19           produces uncertainty in simulation results under certain specific circumstances. For example, poorer  
20           simulation results for daily-scale N<sub>2</sub>O fluxes occurred when precipitation frequency and magnitude were  
21           high (Foltz et al., 2019).

22           Finally, there was uncertainty in the model parameterization. In this study, the parameters were set  
23           based on previous studies and expert knowledge. However, different parameter values could lead to  
24           different simulation results. Sensitivity analysis of the model parameters could help identify the most  
25           critical parameters and their impacts on the simulation results.

26           In summary, this study provided valuable insights into the regional differences in the contribution  
27           of major grain to GHG emissions and water demand in China. However, the uncertainty in the simulation  
28           results needs to be considered and addressed in future studies.

#### 29           **5. Conclusion**

30           This study sought to quantify GHG emissions and crop water demand for six major crops in China:  
31           corn, winter wheat, spring wheat, single-cropping rice, early rice, and late rice, using the DNDC model  
32           and FAO-PM equation. The model was well adapted to multiple farming ecosystems across China using  
33           parameters calibrated for Chinese farm production conditions. Based on the results, the total CO<sub>2</sub>, CH<sub>4</sub>,  
34           and N<sub>2</sub>O emissions of major food crops in China were 372.43 Tg/yr, 11.68 Tg/yr, and 475.56 Gg/yr,  
35           respectively. The total water demand was 473.60 Gm<sup>3</sup> and the national average ET<sub>c</sub> was 435.66 mm. The  
36           water carbon effect varied significantly among crops and was influenced by the area planted, with corn  
37  
38  
39  
40  
41  
42  
43  
44  
45  
46  
47  
48  
49  
50  
51  
52  
53  
54  
55  
56  
57  
58  
59  
60  
61  
62  
63  
64  
65

1       502 identified as the crop with the highest emissions and water demand. Rice crops have greater emission  
2       503 intensity than dry crops, with late rice having the largest GWP of 18,705 kg/ha.  
3

4       504 Significant differences were found in the spatial distribution of GHG emission intensity and water  
5       505 demand in the provincial and agricultural regions. The SC, MLYP, and NEC were identified as hotspot  
6       506 regions for GHG fluxes in China. The hotspots of  $ET_c$  were NASR, SC, and QT. NASR was affected by  
7       507 low mean annual precipitation and had the highest  $ET_c$  (525.91 mm). South China was the only region  
8       508 with high GHG emission fluxes and a high crop water demand.  
9

10      509 For different crops, the intensity of various GHG emissions and the water demand characteristics  
11      510 were found to differ, with  $ET_c$  for late rice in South China being 3.3-fold higher than that for winter  
12      511 wheat. This difference was also influenced by external conditions, such as soil and climate. The effect of  
13      512 soil properties on  $CO_2$  emissions was more significant than that on  $CH_4$  and  $N_2O$  emissions. An increase  
14      513 in the precipitation temperature had a positive effect on GHG emissions. The highest GWP of 18,347.21  
15      514 kg/ha was observed in South China with high temperature and high precipitation. Regional differences  
16      515 in GHG emissions were also identified to be influenced by soil elements. Overall, the increase in soil  
17      516 organic carbon promotes GHG emissions, and soil bulk density plays a suppressive role in GHG  
18      517 emissions. Herein, soil bulk density was identified as the most significant factor affecting GHG emissions.  
19      518  
20  
21  
22  
23  
24  
25  
26  
27  
28  
29  
30  
31  
32  
33  
34  
35  
36  
37  
38  
39  
40  
41  
42  
43  
44  
45  
46  
47  
48  
49  
50  
51  
52  
53  
54  
55  
56  
57  
58  
59  
60  
61  
62  
63  
64  
65

1       **519      Declarations of Competing interest**

2       **520**      The authors declare that they have no known competing financial interests or personal relationships  
3  
4       **521**      that could have appeared to influence the work reported in this paper.

5       **522      Acknowledgements**

6  
7       **523**      This work was jointly supported by the National Natural Science Foundation of China (52122903,  
8  
9       **524**      51979230), Science Fund for Distinguished Young Scholars of Shaanxi Province(2021JC20), Fok Ying-  
10  
11      **525**      Tong Education Foundation (171113) and Cyrus Tang Foundation, China National Postdoctoral Program  
12  
13      **526**      for Innovative Talents (BX20220255).

14       **527      Contributions**

15  
16       **528**      Yihe Tang analyzed the data and wrote the paper; Shikun Sun designed research; all authors  
17  
18       **529**      reviewed the manuscript.

19       **530      Data availability**

20  
21       **531**      Data will be made available on appropriate request.

22       **532**

23  
24  
25  
26  
27  
28  
29  
30  
31  
32  
33  
34  
35  
36  
37  
38  
39  
40  
41  
42  
43  
44  
45  
46  
47  
48  
49  
50  
51  
52  
53  
54  
55  
56  
57  
58  
59  
60  
61  
62  
63  
64  
65

533      **References**

- 534      Allen, R., Pereira, L., Raes, D., Smith, M., Allen, R.G., Pereira, L.S., Martin, S., 1998. Crop  
535      Evapotranspiration: Guidelines for Computing Crop Water Requirements, FAO Irrigation and  
536      Drainage Paper 56. FAO 56. [https://doi.org/doi:  
537      Allen, R.G., Pereira, L.S., 2009. Estimating crop coefficients from fraction of ground cover and height.  
538      \*Irrig Sci\* 28, 17–34. <https://doi.org/10.1007/s00271-009-0182-z>  
539      Della Chiesa, T., Piñeiro, G., Del Grossi, S.J., Parton, W.J., Araujo, P.I., Yahdjian, L., 2022. Higher than  
540      expected N<sub>2</sub>O emissions from soybean crops in the Pampas Region of Argentina: Estimates from  
541      DayCent simulations and field measurements. \*Science of The Total Environment\* 835, 155408.  
542      <https://doi.org/10.1016/j.scitotenv.2022.155408>  
543      Foltz, M.E., Zilles, J.L., Koloutsou-Vakakis, S., 2019. Prediction of N<sub>2</sub>O emissions under different field  
544      management practices and climate conditions. \*Sci Total Environ\* 646, 872–879.  
545      <https://doi.org/10.1016/j.scitotenv.2018.07.364>  
546      Han, D., Yan, D., Xu, X., Gao, Y., 2017. Effects of climate change on spring wheat phenophase and water  
547      requirement in Heihe River basin, China. \*J. Earth Syst. Sci.\* 126, 16.  
548      <https://doi.org/10.1007/s12040-016-0787-6>  
549      IPCC, 2007. In Climate Change 2007: Mitigation. Contribution of Working Group III to the Fourth  
550      Assessment Report of the Intergovernmental Panel on Climate Change. Cambridge University Press,  
551      Cambridge, United Kingdom and New York, NY, USA.  
552      Jia, H., Zhang, T., Yin, X., Shang, M., Chen, F., Lei, Y., Chu, Q., 2019. Impact of Climate Change on the  
553      Water Requirements of Oat in Northeast and North China. \*Water\* 11, 91.  
554      <https://doi.org/10.3390/w11010091>  
555      Koponen, H.T., Duran, C.E., Maljanen, M., Hytonen, J., Martikainen, P.J., 2006. Temperature responses  
556      of NO and N<sub>2</sub>O emissions from boreal organic soil. \*Soil Biol. Biochem.\* 38, 1779–1787.  
557      <https://doi.org/10.1016/j.soilbio.2005.12.004>  
558      Li, C., Frolking, S., Frolking, T.A., 1992. A model of nitrous oxide evolution from soil driven by rainfall  
559      events: 1. Model structure and sensitivity. \*Journal of Geophysical Research: Atmospheres\* 97, 9759–  
560      9776. <https://doi.org/10.1029/92JD00509>  
561      Li, H., Qiu, J., Wang, L., Tang, H., Li, C., Van Ranst, E., 2010. Modelling impacts of alternative farming  
562      management practices on greenhouse gas emissions from a winter wheat–maize rotation system in  
563      China. \*Agriculture, Ecosystems & Environment\* 135, 24–33.  
564      <https://doi.org/10.1016/j.agee.2009.08.003>  
565      Lu, B., Song, L., Zang, S., Wang, H., 2022. Warming promotes soil CO<sub>2</sub> and CH<sub>4</sub> emissions but  
566      decreasing moisture inhibits CH<sub>4</sub> emissions in the permafrost peatland of the Great Xing'an  
567      Mountains. \*Science of The Total Environment\* 829, 154725.  
568      <https://doi.org/10.1016/j.scitotenv.2022.154725>  
569      Lu, S., Bai, X., Li, W., Wang, N., 2019. Impacts of climate change on water resources and grain  
570      production. \*Technol. Forecast. Soc. Chang.\* 143, 76–84.  
571      <https://doi.org/10.1016/j.techfore.2019.01.015>  
572      MEEPRC, 2019. The People's Republic of China Third National Communication on Climate Change.  
573      Ministry of Ecology and Environment of the People's Republic of China \(MEEPRC\), Beijing,  
574      China.](https://doi.org/doi:http://dx.doi.org/)

- 575 Mo, X., Guo, R., Liu, S., Lin, Z., Hu, S., 2013. Impacts of climate change on crop evapotranspiration  
576 with ensemble GCM projections in the North China Plain. *Clim. Change* 120, 299–312.  
577 <https://doi.org/10.1007/s10584-013-0823-3>
- 578 MWRPRC, 2021. *China Water Resources Bulletin*, China Water Resources Bulletin. Ministry of Water  
579 Resources of The People's Republic of China (MWRPRC), Beijing, China.
- 580 NBS, 2020. *China Statistical Yearbook*. National Bureau of Statistics of China (NBS), Beijing, China.
- 581 Niraula, S., Rahman, S., Chatterjee, A., 2018. Temperature response of ammonia and greenhouse gas  
582 emission from manure amended silty clay soil. *Acta Agric. Scand. Sect. B-Soil Plant Sci.* 68, 663–  
583 677. <https://doi.org/10.1080/09064710.2018.1459822>
- 584 Novara, A., Armstrong, A., Gristina, L., Semple, K.T., Quinton, J.N., 2012. Effects of soil compaction,  
585 rain exposure and their interaction on soil carbon dioxide emission. *Earth Surf. Process. Landf.* 37,  
586 994–999. <https://doi.org/10.1002/esp.3224>
- 587 Pereira, L.S., Paredes, P., López-Urrea, R., Hunsaker, D.J., Mota, M., Mohammadi Shad, Z., 2021.  
588 Standard single and basal crop coefficients for vegetable crops, an update of FAO56 crop water  
589 requirements approach. *Agricultural Water Management* 243, 106196.  
590 <https://doi.org/10.1016/j.agwat.2020.106196>
- 591 Piao, S., Ciais, P., Huang, Y., Shen, Z., Peng, S., Li, J., Zhou, L., Liu, H., Ma, Y., Ding, Y., Friedlingstein,  
592 P., Liu, C., Tan, K., Yu, Y., Zhang, T., Fang, J., 2010. The impacts of climate change on water  
593 resources and agriculture in China. *Nature* 467, 43–51. <https://doi.org/10.1038/nature09364>
- 594 Postel, S., Vickers, A., Starke, L., 2004. Boosting Water Productivity. *State of the World* 2004.
- 595 Qiu, R., Li, L., Liu, C., Wang, Z., Zhang, B., Liu, Z., 2022. Evapotranspiration estimation using a  
596 modified crop coefficient model in a rotated rice-winter wheat system. *Agricultural Water  
597 Management* 264, 107501. <https://doi.org/10.1016/j.agwat.2022.107501>
- 598 Saadi, S., Todorovic, M., Tanasijevic, L., Pereira, L.S., Pizzigalli, C., Lionello, P., 2015. Climate change  
599 and Mediterranean agriculture: Impacts on winter wheat and tomato crop evapotranspiration,  
600 irrigation requirements and yield. *Agricultural Water Management, Agricultural Water  
601 Management: Priorities and Challenges* 147, 103–115. <https://doi.org/10.1016/j.agwat.2014.05.008>
- 602 Shcherbak, I., Millar, N., Robertson, G.P., 2014. Global metaanalysis of the nonlinear response of soil  
603 nitrous oxide (N<sub>2</sub>O) emissions to fertilizer nitrogen. *Proc. Natl. Acad. Sci. U. S. A.* 111, 9199–9204.  
604 <https://doi.org/10.1073/pnas.1322434111>
- 605 Shi, Y., Lou, Y., Zhang, Y., Xu, Z., 2021. Quantitative contributions of climate change, new cultivars  
606 adoption, and management practices to yield and global warming potential in rice-winter wheat  
607 rotation ecosystems. *Agricultural Systems* 190. <https://doi.org/10.1016/j.agsy.2021.103087>
- 608 Smith, K.A., 2017. Changing views of nitrous oxide emissions from agricultural soil: key controlling  
609 processes and assessment at different spatial scales. *Eur. J. Soil Sci.* 68, 137–155.  
610 <https://doi.org/10.1111/ejss.12409>
- 611 Smith, W.N., Grant, B.B., Desjardins, R.L., Worth, D., Li, C., Boles, S.H., Huffman, E.C., 2010. A tool  
612 to link agricultural activity data with the DNDC model to estimate GHG emission factors in Canada.  
613 *Agriculture, Ecosystems & Environment* 136, 301–309. <https://doi.org/10.1016/j.agee.2009.12.008>
- 614 Tang, Y., Luan, X., Sun, J., Zhao, J., Yin, Y., Wang, Y., Sun, S., 2021. Impact assessment of climate  
615 change and human activities on GHG emissions and agricultural water use. *Agricultural and Forest  
616 Meteorology* 296, 108218. <https://doi.org/10.1016/j.agrformet.2020.108218>

- 1 Tian, Z., Zhuoran, L., Niu, Y., Li, C., Tu, X., Fan, D., 2014. Simulation of the methane emission in rice  
2 fields in China during the past 40 years by DNDC model and GIS technical. Presented at the 2014  
3 The 3rd International Conference on Agro-Geoinformatics, Agro-Geoinformatics 2014, pp. 1–5.  
4 <https://doi.org/10.1109/Agro-Geoinformatics.2014.6910624>
- 5 UNOHCHR, 2010. Mandate of the Special Rapporteur on the Right to Food. Mission to the People's  
6 Republic of China from 15 to 23 December 2010: Preliminary Observations and Conclusions.  
7 United Nations Office of the High Commissioner for Human Rights, Beijing, China.
- 8 Wang, B., Neue, H.U., Samonte, H.P., 1997. The effect of controlled soil temperature on diel CH<sub>4</sub>  
9 emission variation. Chemosphere 35, 2083–2092. [https://doi.org/10.1016/S0045-6535\(97\)00257-9](https://doi.org/10.1016/S0045-6535(97)00257-9)
- 10 Wang, Z., Zhang, X., Liu, L., Wang, S., Zhao, L., Wu, X., Zhang, W., Huang, X., 2021. Estimates of  
11 methane emissions from Chinese rice fields using the DNDC model. Agric. For. Meteorol. 303,  
12 108368. <https://doi.org/10.1016/j.agrformet.2021.108368>
- 13 Wang, Z., Zhang, X., Liu, L., Wang, S., Zhao, L., Wu, X., Zhang, W., Huang, X., 2020. Inhibition of  
14 methane emissions from Chinese rice fields by nitrogen deposition based on the DNDC model.  
15 Agricultural Systems 184, 102919. <https://doi.org/10.1016/j.agsy.2020.102919>
- 16 Yan, F., Zhang, F., Fan, X., Fan, J., Wang, Y., Zou, H., Wang, H., Li, G., 2021. Determining irrigation  
17 amount and fertilization rate to simultaneously optimize grain yield, grain nitrogen accumulation  
18 and economic benefit of drip-fertigated spring maize in northwest China. Agric. Water Manage.  
19 243, 106440. <https://doi.org/10.1016/j.agwat.2020.106440>
- 20 Yan, W., Zhong, Y., Liu, W., Shangguan, Z., 2021. Asymmetric response of ecosystem carbon  
21 components and soil water consumption to nitrogen fertilization in farmland. Agric. Ecosyst.  
22 Environ. 305, 107166. <https://doi.org/10.1016/j.agee.2020.107166>
- 23 Yang, J., Jia, X., Ma, H., Chen, X., Liu, J., Shangguan, Z., Yan, W., 2022. Effects of warming and  
24 precipitation changes on soil GHG fluxes: A meta- analysis. Sci. Total Environ. 827, 154351.  
25 <https://doi.org/10.1016/j.scitotenv.2022.154351>
- 26 Yang, P., Reijneveld, A., Lerink, P., Qin, W., Oenema, O., 2022. Within-field spatial variations in subsoil  
27 bulk density related to crop yield and potential CO<sub>2</sub> and N<sub>2</sub>O emissions. CATENA 213, 106156.  
28 <https://doi.org/10.1016/j.catena.2022.106156>
- 29 Yang, Y., Liu, L., Zhang, F., Zhang, X., Xu, W., Liu, X., Li, Y., Wang, Z., Xie, Y., 2021. Enhanced nitrous  
30 oxide emissions caused by atmospheric nitrogen deposition in agroecosystems over China. Environ.  
31 Sci. Pollut. Res. 28, 15350–15360. <https://doi.org/10.1007/s11356-020-11591-5>
- 32 Ye, R., Espe, M.B., Linquist, B., Parikh, S.J., Doane, T.A., Horwath, W.R., 2016. A soil carbon proxy to  
33 predict CH<sub>4</sub> and N<sub>2</sub>O emissions from rewetted agricultural peatlands. Agric. Ecosyst. Environ. 220,  
34 64–75. <https://doi.org/10.1016/j.agee.2016.01.008>
- 35 Zhang, F., Qi, J., Li, F.M., Li, C.S., Li, C.B., 2010. Quantifying nitrous oxide emissions from Chinese  
36 grasslands with a process-based model. Biogeosciences 7, 2039–2050. <https://doi.org/10.5194/bg-7-2039-2010>
- 37 Zhang, H., Deng, Q., Schadt, C.W., Mayes, M.A., Zhang, D., Hui, D., 2021. Precipitation and nitrogen  
38 application stimulate soil nitrous oxide emission. Nutr. Cycl. Agroecosyst. 120, 363–378.  
39 <https://doi.org/10.1007/s10705-021-10155-4>
- 40 Zhang, Jingting, Tian, H., Shi, H., Zhang, Jingfang, Wang, X., Pan, S., Yang, J., 2020. Increased  
41 greenhouse gas emissions intensity of major croplands in China: Implications for food security and  
42
- 43
- 44
- 45
- 46
- 47
- 48
- 49
- 50
- 51
- 52
- 53
- 54
- 55
- 56
- 57
- 58
- 59
- 60
- 61
- 62
- 63
- 64
- 65

1 659 climate change mitigation. Global Change Biology 26, 6116–6133.  
2 660 <https://doi.org/10.1111/gcb.15290>  
3 661 Zhao, Q., Brocks, S., Lenz-Wiedemann, V.I.S., Miao, Y., Zhang, F., Bareth, G., 2017. Detecting spatial  
4 662 variability of paddy rice yield by combining the DNDC model with high resolution satellite images.  
5 663 Agricultural Systems 152, 47–57. <https://doi.org/10.1016/j.agrsy.2016.11.011>  
6 664 Zheng, Y., 2015. Research on the Spatial-temporal distribution of growth period of main grain crops and  
7 665 its change in China. Central China Normal University, Hubei, China.  
8 666  
9 667  
10  
11  
12  
13  
14  
15  
16  
17  
18  
19  
20  
21  
22  
23  
24  
25  
26  
27  
28  
29  
30  
31  
32  
33  
34  
35  
36  
37  
38  
39  
40  
41  
42  
43  
44  
45  
46  
47  
48  
49  
50  
51  
52  
53  
54  
55  
56  
57  
58  
59  
60  
61  
62  
63  
64  
65

1  
2  
3  
4  
5  
6  
7  
8  
9  
10  
11  
12  
13  
14  
15  
16  
17  
18  
19  
20  
21  
22  
23  
24  
25  
26  
27  
28  
29  
30  
31  
32  
33  
34  
35  
36  
37  
38  
39  
40  
41  
42  
43  
44  
45  
46  
47  
48  
49  
50  
51  
52  
53  
54  
55  
56  
57  
58  
59  
60  
61  
62  
63  
64  
65

**Supplementary Information for:**

**Assessing the impact of climate and crop diversity on regional greenhouse gas emissions and water demand of cropland**

**Supplementary Information Figures**

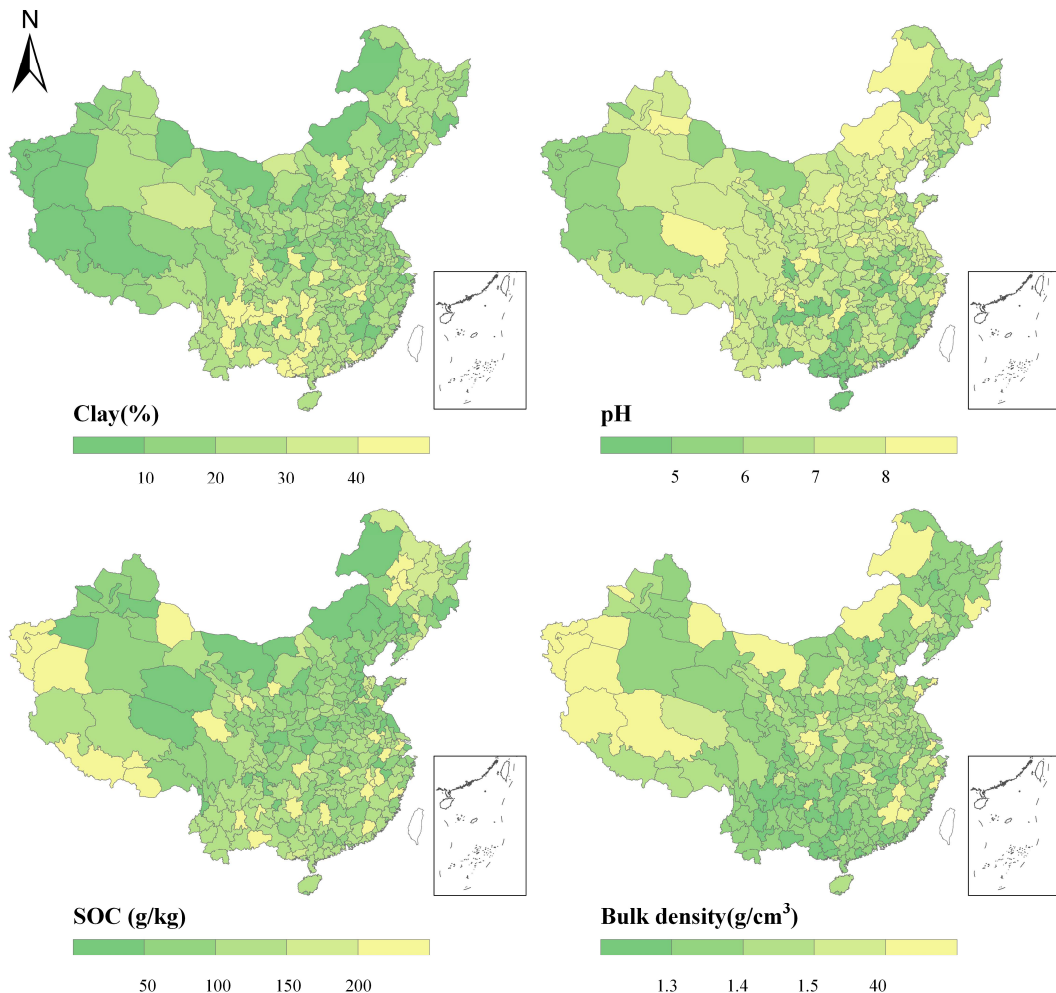


**Fig. S1 Spatial distribution map of soil properties (a.soil clay content, b.soil PH, c.soil organic carbon content (SOC) ,d.soil bulk density)**

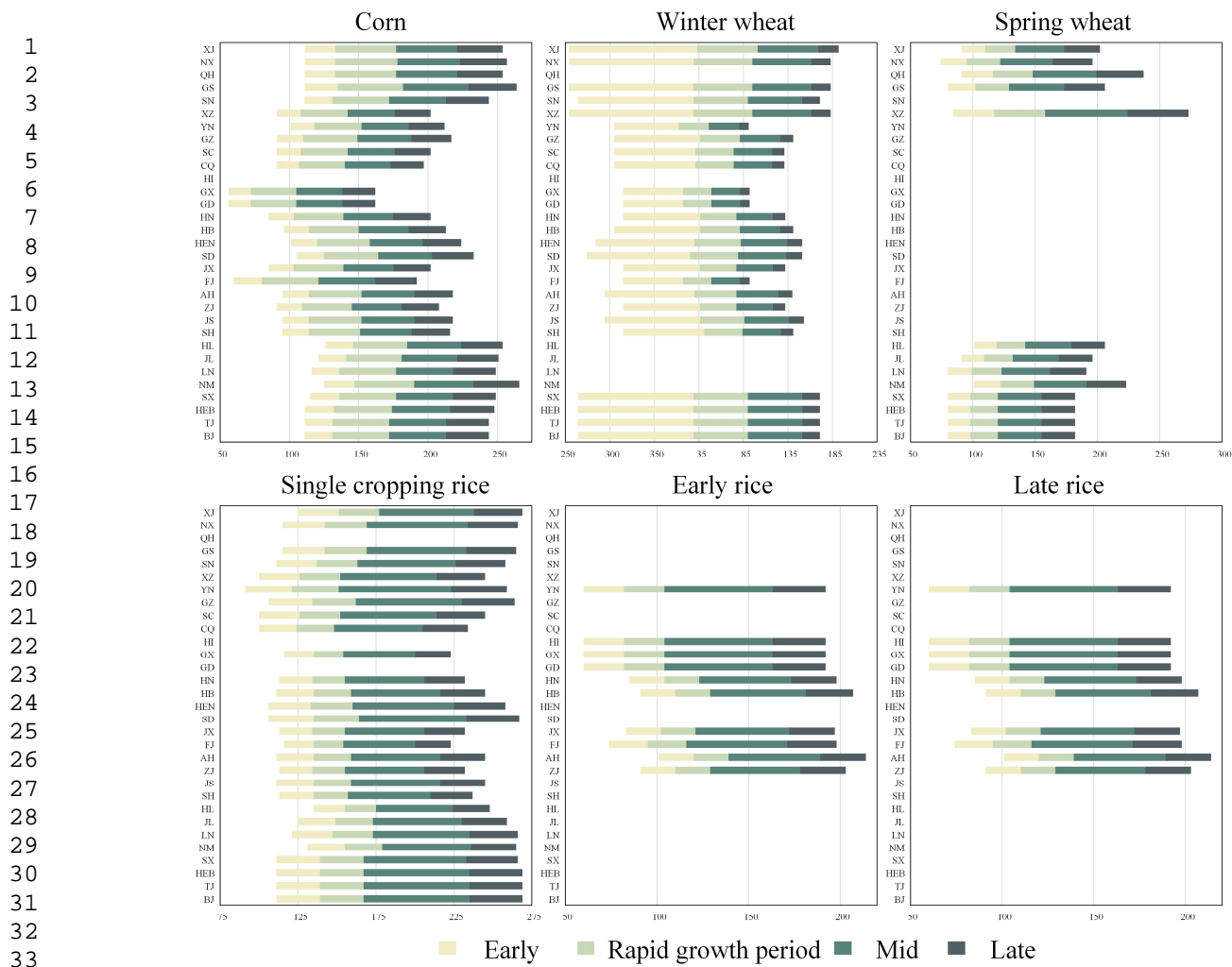


Fig.S2 Provincial crop growth period(The abscissa is day of year)

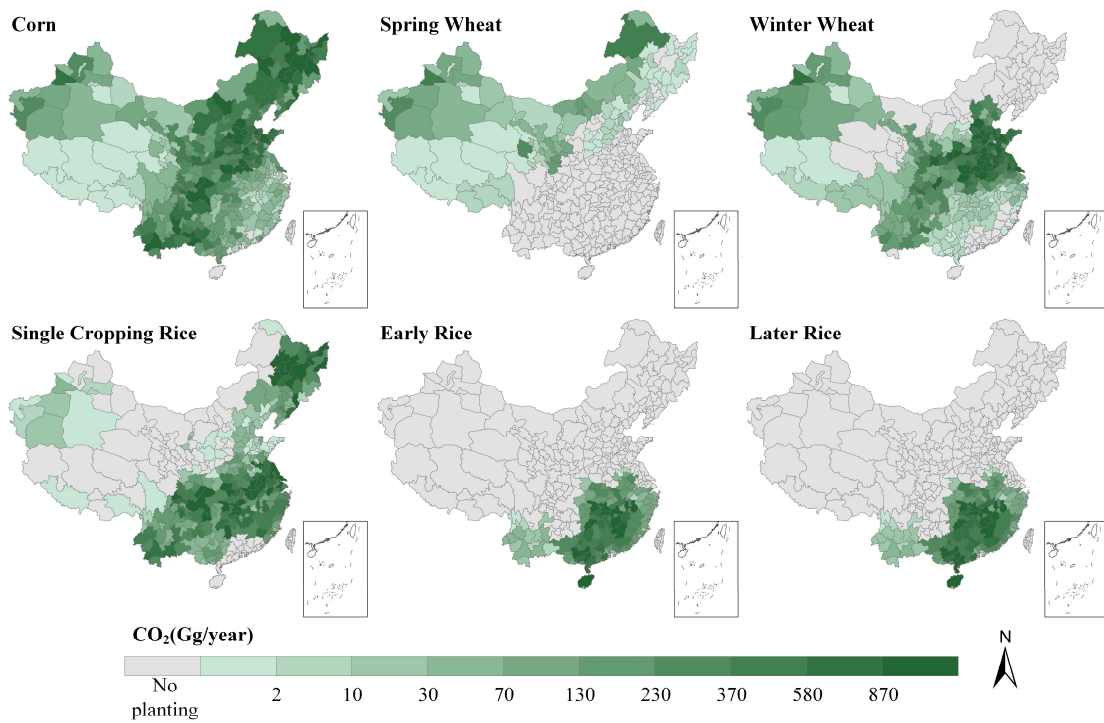


Fig.S3 Total annual CO<sub>2</sub> emissions of each crop

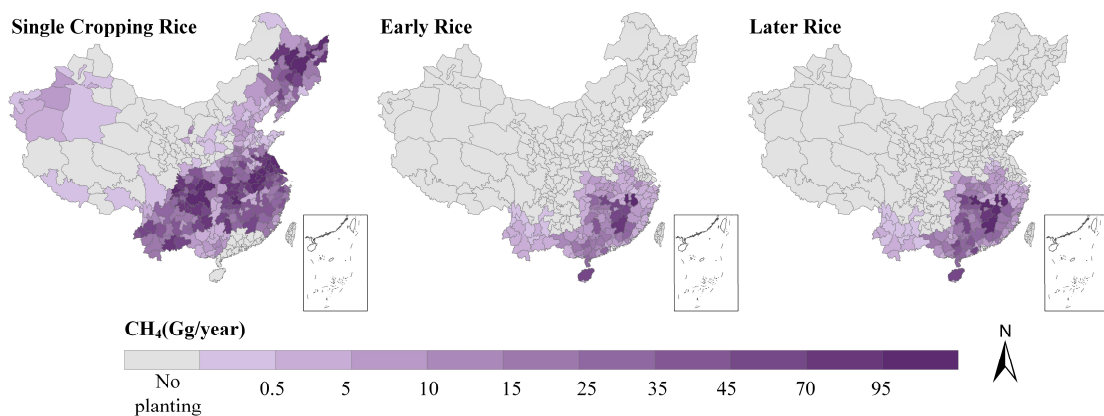


Fig.S4 Total annual CH<sub>4</sub> emissions of each crop

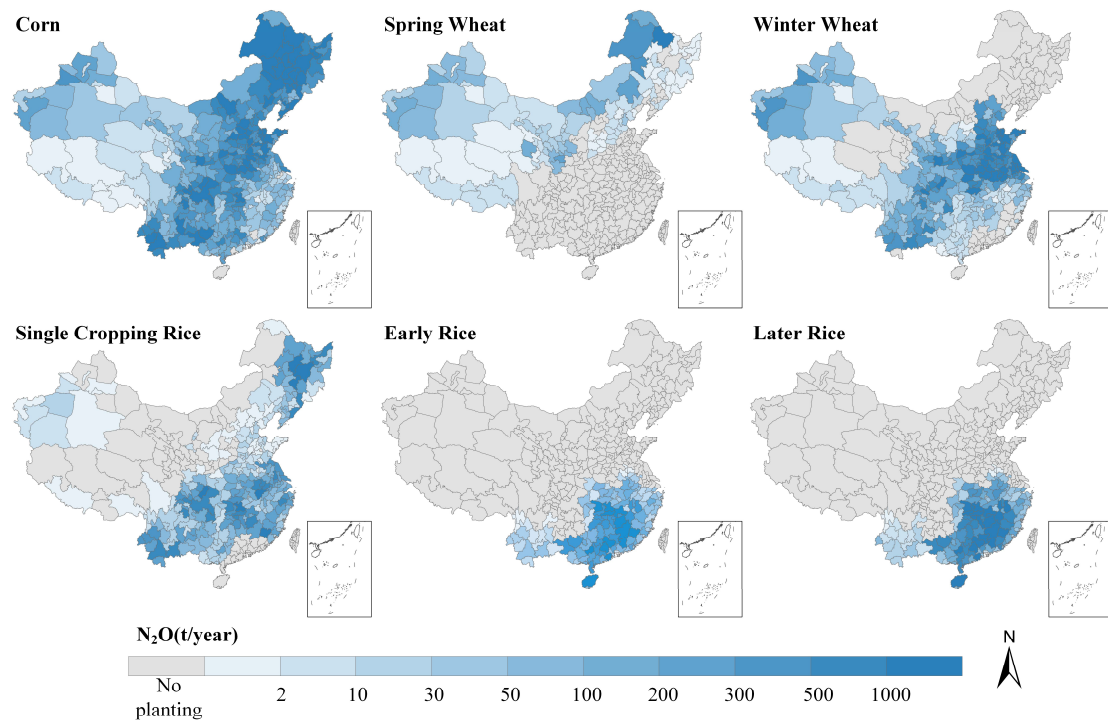


Fig.S5 Total annual N<sub>2</sub>O emissions of each crop

1                   **Supplementary Information tables**

2                   Table S1 Input parameters required for regional simulation with DNDC

Items	Input parameters
<b>Climate</b>	Temperature, precipitation, rainfall N concentration
<b>Soil</b>	SOC, soil texture, pH, bulk density
<b>Crop parameters</b>	Acreage, maximum yield, thermal degree days, water demand, growing degree days
<b>Management</b>	Planting date, harvest date, fertilizer application rate, film mulch, manure amendment, tillage, residue incorporation

23                   Table S2 Parameterized range of major crop parameters

Crop	Variables	Database
Corn	Max grain yield (kgC/ha)	2000-5000
	Ratio of grain organs	0.25-0.4
	TDD (°C)	1800-2100
Wheat	Max grain yield (kgC/ha)	500-2500
	Ratio of grain organs	0.25-0.45
	TDD (°C)	1600-1900
Rice	Max grain yield (kgC/ha)	2000-5000
	Ratio of grain organs	0.2-0.4
	TDD (°C)	1900-2200

38                   Note: Crop parameters for winter and spring wheat varied across simulation units, although the range of  
39                   variation remained consistent. Similarly, this held true for early, late, and single-season rice.

42                   Table S3 Basic information on validation points

Crop	Province	longitude and latitude	pH	Bulk density ( $\text{g}\cdot\text{cm}^{-3}$ )	clay	SOC ( $\text{g}\cdot\text{kg}^{-1}$ )	year	References
Corn	Cangzhou, Hebei	37°63'N, 116°44'E	7.4	1.68	0.11	12.7	2019-2020	(Wang et al., 2022)
Corn	Quzhou, Hebei	36°52'N, 115°01'E	7.72	1.37		12.6	2009-2013	(Abdalla et al., 2022)
Corn	Quzhou, Hebei	36°31'N, 115°00'E	7.97	1.38	/	8.5	2006-2006	(Li et al., 2010)
Corn	Quzhou, Hebei	36°52'N, 115°01'E	8.3	1.36	/	14.2	2012	(Abdalla et al., 2020;

1										Song et al., 2018)
2										(Li et al., 2012)
3		Corn	Dalian, Liaoning	39°30'N, 121°45'E	7.6	1.38		12.3	2009	
4		Corn	Yangling, Shanxi	34°17'N, 108°00'E	8.6	1.34	0.32	15.1	2015-2016	(Lv et al., 2020)
5		Corn	Yangling, Shanxi	34°20'N, 108°24'E	8.2	1.37	0.17	8.14	2013-2016	(Chen et al., 2019)
6		Corn	Yongji, Shanxi	34°55'N, 110°42'E	8.7	1.17	0.32	11.3	2007-2010	(Zhang et al., 2015)
7		Corn	Yongji, Shanxi	36°58'N, 117°59'E	8.3	1.42	0.17	1.05	2008-2010	(Zhang et al., 2015)
8		Corn	Yongji, Shanxi	36°58'N, 117°59'E	8.3	1.32	0.19	8.5	2004-2007	(Zhang et al., 2015)
9		Corn	Tingzhou, Beijing	39°41'N, 116°41'E	7.8	1.57	0.32	11.06	2013-2015	(Chi et al., 2020)
10		Corn	Cangzhou, Hebei	37°63'N, 116°44'E	7.4	1.68	0.11	12.7	2018-2020	(Wang et al., 2022)
11		Wheat	Cangzhou, Hebei	37°63'N, 116°44'E	7.4	1.68	0.11	12.7	2018-2020	(Wang et al., 2022)
12		Wheat	Changshu, Jiangsu	31°32'N, 120°41'E	7.7	1.2	/	20.1	2012-2014	(Xia et al., 2016)
13		Wheat	Quzhou, Hebei	36°52'N, 115°01'E	7.72	1.37		12.6	2009-2013	(Abdalla et al., 2022)
14		Wheat	Quzhou, Hebei	36°31'N, 115°00'E	7.97	1.38	/	8.5	2005-2006	(Li et al., 2010)
15		Wheat	Quzhou, Hebei	36°52'N, 115°01'E	8.3	1.36	/	14.2	2012-2013	(Abdalla et al., 2020; Song et al., 2018)
16		Wheat	Yangling, Shanxi	34°17'N, 108°00'E	8.6	1.34	0.32	15.1	2015-2016	(Lv et al., 2020)
17		Wheat	Yangling, Shanxi	34°20'N, 108°24'E	8.2	1.37	0.17	8.14	2013-2016	(Chen et al., 2019)
18		Wheat	Yongji, Shanxi	34°55'N, 110°42'E	8.7	1.17	0.32	11.3	2007-2010	(Zhang et al., 2015)
19		Wheat	Yongji, Shanxi	36°58'N, 117°59'E	8.3	1.42	0.17	1.05	2008-2010	(Zhang et al., 2015)
20		Wheat	Yongji, Shanxi	36°58'N, 117°59'E	8.3	1.32	0.19	8.5	2004-2007	(Zhang et al., 2015)
21		Rice	Jian, Jiangxi	26°44'N, 115°04'E	5.00	1.31	0.14	10.0	2012-2014	(Sun et al., 2023)
22		Rice	Nanjing, Jiangsu	32°14'N, 118°42'E	6.57	1.36	0.26	25.0	2015-2016	(Chen et al., 2020)

1	Rice	Jiamusi, Heilongjiang	47°35'N, 133°31'E	5.61	0.98	0.41	27.7	2004	(Zhang et al., 2011)
2	Rice	Huaiyuan, Anhui	33°04'N, 117°05'E	7.5	1.45	0.19	16.0	2011-2012	(Zhang et al., 2022)
3	Rice	Shanghai	30°53'N, 121°23'E	7.6	1.40	0.27	13.7	2013-2016	(Zhang et al., 2019)
4	Rice	Suihua, Heilongjiang	46°57'N, 127°40'E	6.4	1.26	0.21	41.8	2017	(Nie et al., 2019)
5	Rice	Changshu, Jiangsu	31°32'N, 120°41'E	7.7	1.2	/	20.1	2013-2015	(Xia et al., 2016)
6	Rice	Kunshan, Jiangsu	34°63'N, 121°05'E	7.4	1.53	0.89	30.3	2003-2005	(Wu and Zhang, 2014)
7	Rice	Shanghai	30°53'N, 121°23'E	7.6	1.4	/	13.7	2013-2014	(Sun et al., 2016)
8									
9									
10									
11									
12									
13									
14									
15									
16									
17									
18									
19									
20									
21									
22									
23									
24									
25									
26									
27									
28									
29									
30									
31									
32									
33									
34									
35									
36									
37									
38									
39									
40									
41									
42									
43									
44									
45									
46									
47									
48									
49									
50									
51									
52									
53									
54									
55									
56									
57									
58									
59									
60									
61									
62									
63									
64									
65									

Table S4 Agricultural regional division and abbreviations of provincial administrative regions

Agricultural region			Province	
<b>Northeast China Plain</b>		NEC	Liaoning	LN
			Jilin	JL
			Heilongjiang	HL
<b>Yunnan-Guizhou Plateau</b>		YGP	Guizhou	GZ
			Yunnan	YN
			Guangxi	GX
<b>Northern arid and semiarid region</b>		NASR	Gansu	GS
			Ningxia	NX
			Xinjiang	XJ
			NeiMengGu	NM
<b>Southern China</b>		SC	Guangdong	GD
			Hainan	HI
			Fujian	FJ
<b>Sichuan Basin and surrounding regions</b>		SCB	Chongqing	CQ
			Sichuan	SC
<b>Middle-lower Yangtze Plain</b>		MLYP	Hebei	HB
			Hunan	HN
			Jiangxi	JX
			Shanghai	SH
			Jiangsu	JS
<b>Qinghai Tibet Plateau</b>		QTP	Zhejiang	ZJ
			Anhui	AH
			Xizang	XZ
<b>Loess Plateau</b>		LP	Qinghai	QH
			Shaanxi	SN

---

		Shanxi	SX
1		Beijing	BJ
2		Tianjin	TJ
3		Hebei	HEB
4	<b>Huang-Huai-Hai Plain</b>	HHHP	
5		Henan	HEN
6		Shandong	SD
7			
8			
9			
10			
11			
12			
13			
14			
15			
16			
17			
18			
19			
20			
21			
22			
23			
24			
25			
26			
27			
28			
29			
30			
31			
32			
33			
34			
35			
36			
37			
38			
39			
40			
41			
42			
43			
44			
45			
46			
47			
48			
49			
50			
51			
52			
53			
54			
55			
56			
57			
58			
59			
60			
61			
62			
63			
64			
65			

---

Table S3 Modified crop coefficients

Province	City ID	Corn		Spring wheat		Winter wheat		Single cropping rice		Early rice		Late rice				
		Keini	Kcmid	Kcend	Keini	Kemid	Kcend	Keini	Kcmid	Kcend	Keini	Kcmid	Kcend	Keini	Kcmid	Kcend
BJ	110000	0.38	1.25	0.41	0.29	1.19	0.34	0.65	1.25	0.38	1.11	1.24	0.76	0	0	0
TJ	120000	0.39	1.23	0.38	0.29	1.19	0.33	0.64	1.26	0.39	1.12	1.22	0.73	0	0	0
HEB	130100	0.34	1.22	0.39	0.32	1.17	0.32	0.60	1.22	0.42	1.09	1.21	0.75	0	0	0
HEB	130800	0.36	1.18	0.35	0.29	1.14	0.29	0.63	1.21	0.33	1.09	1.18	0.70	0	0	0
HEB	130700	0.34	1.22	0.39	0.32	1.17	0.32	0.60	1.22	0.42	1.09	1.21	0.75	0	0	0
HEB	130300	0.37	1.21	0.38	0.29	1.18	0.31	0.62	1.22	0.36	1.11	1.20	0.74	0	0	0
HEB	130200	0.36	1.19	0.32	0.28	1.16	0.30	0.61	1.20	0.34	1.10	1.19	0.71	0	0	0
HEB	131000	0.38	1.25	0.41	0.29	1.19	0.34	0.65	1.25	0.38	1.11	1.24	0.76	0	0	0
HEB	130600	0.35	1.22	0.30	0.28	1.15	0.31	0.61	1.20	0.39	1.09	1.21	0.70	0	0	0
HEB	130900	0.34	1.22	0.39	0.32	1.17	0.32	0.60	1.22	0.42	1.09	1.21	0.75	0	0	0
HEB	131100	0.33	1.21	0.32	0.30	1.13	0.31	0.61	1.18	0.41	1.07	1.20	0.75	0	0	0
HEB	130500	0.34	1.22	0.39	0.32	1.17	0.32	0.60	1.22	0.42	1.09	1.21	0.75	0	0	0
HEB	130400	0.38	1.27	0.43	0.34	1.22	0.38	0.66	1.26	0.45	1.12	1.25	0.78	0	0	0
SX	140100	0.38	1.20	0.34	0.30	1.18	0.31	0.62	1.23	0.39	1.11	1.20	0.70	0	0	0
SX	140200	0.39	1.21	0.41	0.28	1.12	0.28	0.62	1.25	0.38	1.12	1.21	0.75	0	0	0
SX	140300	0.39	1.21	0.41	0.28	1.12	0.28	0.62	1.25	0.38	1.12	1.21	0.75	0	0	0
SX	140400	0.39	1.21	0.41	0.28	1.12	0.28	0.62	1.25	0.38	1.12	1.21	0.75	0	0	0
SX	140500	0.39	1.21	0.41	0.28	1.12	0.28	0.62	1.25	0.38	1.12	1.21	0.75	0	0	0
SX	140600	0.37	1.20	0.42	0.28	1.12	0.32	0.61	1.24	0.38	1.10	1.22	0.76	0	0	0
SX	140700	0.38	1.20	0.34	0.30	1.18	0.31	0.62	1.23	0.39	1.11	1.20	0.70	0	0	0
SX	140800	0.31	1.19	0.38	0.29	1.19	0.34	0.55	1.18	0.40	1.05	1.19	0.73	0	0	0
SX	140900	0.37	1.23	0.44	0.31	1.18	0.32	0.64	1.25	0.42	1.10	1.23	0.78	0	0	0
SX	141000	0.32	1.21	0.40	0.30	1.19	0.32	0.58	1.21	0.39	1.07	1.21	0.75	0	0	0

























23	XJ	654200	0.35	1.25	0.47	0.33	1.11	0.26	0.60	1.18	0.38	1.08	1.24	0.80	0	0	0	0	0
24	XJ	654300	0.36	1.22	0.46	0.32	1.12	0.22	0.59	1.19	0.37	1.08	1.24	0.79	0	0	0	0	0

**Declaration of interests**

The authors declare that they have no known competing financial interests or personal relationships that could have appeared to influence the work reported in this paper.

The authors declare the following financial interests/personal relationships which may be considered as potential competing interests:

Shikun Sun reports financial support was provided by the National Natural Science Foundation of China. Shikun Sun reports financial support was provided by Science Fund for Distinguished Young Scholars of Shaanxi Province. Shikun Sun reports financial support was provided by Fok Ying-Tong Education Foundation. Yali Yin reports financial support was provided by China National Postdoctoral Program for Innovative Talents. Shikun Sun reports financial support was provided by Cyrus Tang Foundation.